

Identification of nesfatin-1 as a satiety molecule in the hypothalamus

Shinsuke Oh-I¹, Hiroyuki Shimizu¹, Tetsuro Satoh¹, Shuichi Okada¹, Sachika Adachi², Kinji Inoue², Hiroshi Eguchi³, Masanori Yamamoto³, Toshihiro Imaki¹, Koushi Hashimoto¹, Takafumi Tsuchiya¹, Tsuyoshi Monden¹, Kazuhiko Horiguchi¹, Masanobu Yamada¹ & Masatomo Mori¹

¹Department of Medicine and Molecular Science, Gunma University Graduate School of Medicine, Showa-machi, Maebashi 371-8511, Japan. ²Department of Regulation Biology, Saitama University, Shimo-okubo, Saitama 378-8570, Japan, ³Pharmaceutical Discovery Research Laboratory, Teijin Pharma Limited, Asahigaoka, Hino 191-8512, Japan.

The brain hypothalamus contains certain secreted molecules that are important in regulating feeding behaviour¹⁻³. Here we show that nesfatin, corresponding to NEFA/nucleobindin2 (NUCB2), a secreted protein of unknown function, is expressed in the appetite-control hypothalamic nuclei in rats.

Intracerebroventricular (i.c.v.) injection of NUCB2 reduces feeding. Rat cerebrospinal fluid contains nesfatin-1, an amino-terminal fragment derived from NUCB2, and its expression is decreased in the hypothalamic paraventricular nucleus under starved conditions. I.c.v. injection of nesfatin-1 decreases food intake in a dose-dependent manner, whereas injection of an antibody neutralizing nesfatin-1 stimulates appetite. In contrast, i.c.v. injection of other possible fragments processed from NUCB2 does not promote satiety, and conversion of NUCB2 to nesfatin-1 is necessary to induce feeding suppression. Chronic i.c.v. injection of nesfatin-1 reduces body weight, whereas rats gain body weight after chronic i.c.v. injection of antisense morpholino oligonucleotide against the gene encoding NUCB2. Nesfatin-1-induced anorexia occurs in Zucker rats with a leptin receptor mutation, and an anti-nesfatin-1 antibody does not block leptin-induced anorexia. In contrast, central injection of α -melanocyte-stimulating hormone elevates NUCB2 gene expression in the paraventricular nucleus, and satiety by nesfatin-1 is abolished by an antagonist of the melanocortin-3/4 receptor. We identify nesfatin-1 as a satiety molecule that is associated with melanocortin signalling in the hypothalamus.

We attempted to identify any new appetite-regulating molecules by using a subtraction-cloning assay of peroxisome proliferator-activated receptor- γ activator (troglitazone)-stimulated genes in SQ-5 cells. First, we used a computer-based

program (Signal Peptide Prediction, http://bioinformatics.leeds.ac.uk/prot_analysis/Signal.html) to search for a signal peptide in the coding region of each of the 596 genes cloned in this assay. As most hypothalamic secreted molecules also exist in peripheral adipose tissue⁴, we examined whether the genes cloned were expressed in both brain medulloblastoma (HTB185) and 3T3-L1 adipocyte cells. Nine genes meeting these criteria were identified, and the expression of one gene among those identified was profoundly stimulated by troglitazone in SQ-5 cells (Supplementary Fig. 1). Sequencing demonstrated that this complementary DNA fragment corresponds to the 5'-untranslated region of the gene encoding DNA binding/EF-hand/acidic protein (NEFA) or NUCB2. NUCB2 is composed of a signal peptide of 24 amino acids and a protein structure containing 396 amino acids⁵. The homology of the amino-acid sequence of NUCB2 is highly conserved in humans, mice and rats (87.4% homology to humans and 95.7% to mice). Because NUCB2 belongs to a homologous gene family with nucleobindin1 (NUCB1)⁶, these two genes might have arisen from a single EF-hand ancestor⁷. NUCB2 and NUCB1 are secreted proteins⁵⁻⁸ but their function remains unknown, although these proteins have been suggested to contribute to bone mineralization and antibody production^{9,10}.

Troglitazone does not cross the blood–brain barrier to alter feeding behaviour¹¹ and does not change body weights in rodents (Supplementary Fig. 2), but the present findings encouraged further investigation into whether the protein deduced from this identified gene is present in the hypothalamus. To address this issue, an anti-NUCB2 antibody (termed NUCB2 Ab-L) was used to perform immunohistochemical analyses in rats. This antibody recognizes the whole structure of NUCB2, and its detection was not absorbed by the addition of appetite-regulating peptides (Supplementary Fig. 3). NUCB2 was expressed in the hypothalamic areas (Fig. 1a–d), namely the arcuate nucleus, paraventricular nucleus (PVN) and supraoptic nucleus, the lateral hypothalamic area and the zona incerta, which regulate feeding, and also in the nucleus tract solitarius (data not shown). Preincubation of the cognate peptide with NUCB2 Ab-L abolished staining (data not shown). Analysis of *in situ* hybridization demonstrated that the gene encoding NUCB2 is expressed in the same hypothalamic nuclei as those shown by the immunohistochemistry (Fig. 1e). We next identified that i.c.v. injection of recombinant protein of NUCB2 decreased food

intake (Fig. 1f, g), but no apparent behavioural changes including increased locomotion or narcolepsy were noted during the experiments. Conversely, i.c.v. injection of IgG from NUCB2 Ab-L stimulated feeding, compared with that induced by control IgG (Supplementary Fig. 4). These results indicate that this protein is a hypothalamic endogenous molecule that induces anorexia. We therefore refer to this protein as nesfatin (for NEFA/nucleobindin2-encoded satiety- and fat-influencing protein).

Post-translational processing of a prohormone produces several fragments or peptides through cleavage at specific sites by prohormone convertases (PCs)¹², and rat NUCB2/nesfatin possesses potential cleavage sites that are flanked by a pair of basic amino acids, Lys-Arg or Arg-Arg (Supplementary Fig. 5). The ProP 1.0 prediction server¹³ predicted these sites and showed the highest score for cleavage at the Lys 83-Arg 84 site, which is conserved among different species⁵⁻⁷. The possible processed fragments were designated as follows; nesfatin-1, residues 1–82; nesfatin-2, residues 85–163; and nesfatin-3, residues 166–396. The structures of nesfatin-2 and nesfatin-3 are characterized by their possessing putative DNA-binding and leucine-zipper sites that bind nucleosomal DNA^{5,6}, but nesfatin-1 does not preserve these sites. We produced two different types of antibody, nesfatin Ab24 and Ab301, which recognized synthetic nesfatin-1 and nesfatin-3, respectively (Supplementary Fig. 5). When monitored by nesfatin-1 ELISA, elution profiles of cerebrospinal fluid extracts on high-performance liquid chromatography showed an apparent peak corresponding to nesfatin-1 peptide (Supplementary Figs 6 and 7), indicating that nesfatin-1 is a secreted fragment. Immunohistochemical analysis with nesfatin Ab24 showed that nesfatin-1 was distributed in the hypothalamic nuclei in a similar manner to that observed for NUCB2 Ab-L (Supplementary Fig. 8) and was present in the cytoplasm, but not the nucleus, of the hypothalamic neurons, where it was co-localized with PC-3/1 and PC-2 (Fig. 1h). Under conditions of starvation for 24 h, NUCB2 gene expression was reduced in the PVN, in which nesfatin-1 concentration was also decreased (Fig. 1i, j). No significant changes were observed in other hypothalamic nuclei.

As a prohormone can be processed to generate bioactive fragments¹⁴, we next estimated the food intake of rats after i.c.v. injection of each of the possible fragments derived from NUCB2. Injection of a synthetic peptide identical to nesfatin-1

decreased food intake in a dose-dependent manner, and the effects continued for 6 h after injection (Fig. 2a, b). In contrast, neither a synthetic peptide corresponding to nesfatin-2, a fragment corresponding to nesfatin-3 nor a fragment corresponding to nesfatin-2/3 affected appetite (Fig. 2c, d). Subsequently, we found that food intake was significantly stimulated after injection of nesfatin Ab24-derived IgG, but not after injection of nesfatin Ab301-derived IgG (Fig. 2e). Finally, we found that although i.c.v. injection of the intermediate form (residues 1–223) of nesfatin retaining wild-type Lys 83-Arg 84 significantly reduced feeding, injection of the mutant form of nesfatin (Ala 83-Ala 84) did not induce anorexia (Fig. 2f–h), indicating that appetite suppression by NUCB2 requires conversion to nesfatin-1.

In the next experiments we estimated chronological changes in rat body weight. In comparison with rats receiving vehicle injection (Fig. 3a, b), rats receiving a continuous i.c.v. injection of nesfatin-1 unfailingly showed decreased food intake and suppressed body weight gain (at Day 10, 30.4 ± 0.3 versus 12.6 ± 0.7 s.e.m. g, respectively). Nesfatin-1 injection also significantly decreased the weights of subcutaneous, epididymal and mesenteric fats, but not that of the gastrocnemius (Supplementary Fig. 9). Conversely, continuous i.c.v. injection of NUCB2 antisense morpholino oligonucleotide diminished the hypothalamic NUCB2 contents (Supplementary Fig. 10) and resulted in a consistent increase in appetite. Initially, body weight gains remained unchanged until 5 days after injection, but significant increases occurred after 6 days (Fig. 3c, d).

There are complex but integrated interconnections among the hypothalamic nuclei in regulating feeding^{1,2,15}. Leptin and pro-opiomelanocortin (POMC)-derived α -melanocyte-stimulating hormone are key anorectic molecules in the hypothalamus^{1–3}. In Zucker rats possessing a leptin receptor mutation¹⁶, significant nesfatin-1-induced satiety occurred (Fig. 4a, b). Previous injection of nesfatin Ab24 eliminated anorexia induced by nesfatin-1, but did not block leptin-induced anorexia (Fig. 4c), indicating a possible lack of involvement of hypothalamic leptin signalling in the induction of anorexia by nesfatin-1. In contrast, central injection of α -melanocyte-stimulating hormone stimulated the expression of the PVN gene encoding NUCB2 (Supplementary Fig. 11), and previous injection of SHU9119, an antagonist specific for the melanocortin 3/4 receptor¹⁷, abolished nesfatin-1-induced satiety (Fig. 4d, e). However, injection of nesfatin-1 did not affect the expression of the genes

encoding POMC, agouti-related peptide, neuropeptide Y or corticotropin-releasing hormone in the arcuate nucleus and PVN (Supplementary Fig. 12), and nesfatin-1 stimulated neither cAMP formation nor calcium influx in cells expressing the melanocortin-3 or -4 receptor (Supplementary Fig. 13). As the melanocortin-4 receptor is distributed widely in several brain regions that are plausibly involved in the coordinated control of feeding and energy expenditure^{15,18,19}, these findings imply the possible involvement of unknown neuronal substances, which are regulated by the melanocortin-4 receptor signaling, in mediating nesfatin-1-induced anorexia. Taken together, the present studies indicate that hypothalamic nesfatin-1 signalling might involve the leptin-independent melanocortin signalling system²⁰.

We have identified a novel anorexigenic nesfatin corresponding to NUCB2 in the hypothalamus that produces a secreted fragment, nesfatin-1. At the carboxy terminus matching the nesatin-2/3 fragment, NUCB2 possesses archetypal motifs, namely possible calcium-binding and DNA-binding sites⁵⁻⁷. The C-terminal region also binds other molecules²¹. However, the present findings indicate that this C terminus is not involved in feeding regulation. In contrast, nesfatin-1 located in the N terminus of NUCB2 was indispensable to the induction of satiety, and conversion of NUCB2 to nesfatin-1 was essential to induce its activity *in vivo*.

The present findings indicate that nesfatin-1 might be a useful target for the development of drug therapies to treat obese persons.

Methods

Further details are provided in Supplementary Information.

Subtraction-cloning assay

With the use of a polymerase chain reaction (PCR)-based subtraction cloning kit²², the troglitazone (100 μ M)-stimulated genes of SQ-5 cells derived from lung carcinomas, which express leptin and its receptor²³, were identified.

Proteins and substances

A cDNA encoding full-length mouse NUCB2 was subcloned into pMAL-c2x to yield a fusion protein with maltose binding protein in *Escherichia coli*. The intermediate forms of nesfatin retaining the wild-type motif Lys 83-Arg 84 or the mutant Lys 83-Arg 84→Ala 83-Ala 84 (mutations generated by the PCR method) were constructed

as glutathione *S*-transferase fusion proteins with a histidine tag in *E. coli* transfected with the pET41a(+) vector. Peptides for rat nesfatin-1 and nesfatin-2 were synthesized by Yanaihara Institute, Inc.

Antibodies

Antibodies were generated in rabbits against amino-acid sequences of rat NUCB2: Ab-L against residues 117–128, Ab24 against residues 24–38, and Ab301 against residues 301–314. A Cys residue was added to the C terminus of each peptide.

Animal experiments

Without anaesthesia, the test substance (5 µl) was injected into the third ventricle of the brain in adult male Wistar rats weighing 200–250 g, as described previously²⁴. The experiments involving i.c.v. bolus injection were started 30 min before the beginning of the dark cycle (lighting from 6:00 to 18:00), and the experiments for IgG injection were started at 10:00 unless otherwise specified. Zucker obese rats were purchased from Charles River Laboratory.

Statistical analysis was performed by analysis of variance, unless otherwise mentioned.

Received 8 June 2006; accepted 11 August 2006; doi:10.1038/nature05162.

Published online XXX 2006.

1. Friedman, J. F. & Halaas, J. L. Leptin and the regulation of body weight in mammals. *Nature* **395**, 763–770 (1998).
2. Schwartz, M. W. *et al.* Central nervous system control of food intake. *Nature* **404**, 661–671 (2000).
3. Stanley, S., Wynne, K., McGowan, B. & Bloom, S. Hormonal regulation of food intake. *Physiol. Rev.* **85**, 1131–1158 (2005).
4. Shimizu, H. & Mori, M. The brain–adipose axis: a review of involvement of molecules. *Nutr. Neurosci.* **8**, 7–20 (2005).
5. Barnikol-Watanabe, S. *et al.* Human protein NEFA, a novel DNA binding/EF-hand/leucine zipper protein. Molecular cloning and sequence analysis of the cDNA, isolation and characterization of the protein. *Biol. Chem. Hoppe-Seyler* **375**, 497–512 (1994).

6. Miura, K., Titani, K., Kurisawa, Y. & Kanai, Y. Molecular cloning of nucleobindin, a novel DNA-binding protein that contains both a signal peptide and a leucine zipper structure. *Biochem. Biophys. Res. Commun.* **187**, 375–380 (1992).
7. Karabinos, A. *et al.* The divergent domains of the NEFA and nucleobindin proteins are derived from an EF-hand ancestor. *Mol. Biol. Evol.* **13**, 990–998 (1996).
8. Lavoie, C., Meerloo, T., Lin, P. & Farquhar, M. G. Calnuc, an EF-hand Ca²⁺-binding protein, is stored and processed in the golgi and secreted by the constitutive-like pathway in AtT20 cells. *Mol. Endocrinol.* **16**, 2462–2474 (2002).
9. Petersson, U. *et al.* Nucleobindin is produced by bone cells and secreted into the osteoid, with a potential role as a modulator of matrix maturation. *Bone* **34**, 949–960 (2004).
10. Kanai, Y. *et al.* Natural occurrence of Nuc in the sera of autoimmune-prone MRL/lpr mice. *Biochem. Biophys. Res. Commun.* **196**, 729–736 (1993).
11. Jia, D. M. *et al.* Troglitazone prevents and reverses dyslipidemia, insulin secretory defects, and histologic abnormalities in a rat model of naturally occurring obese diabetes. *Metabolism* **49**, 1167–1175 (2000).
12. Zhou, A., Webb, G., Zhu, X. & Steiner, D. F. Proteolytic processing in the secretory pathway. *J. Biol. Chem.* **274**, 20745–20748 (1999).
13. Duckert, P., Brunak, S. & Blom, N. Prediction of protein convertase cleavage sites. *Protein Eng. Design Select.* **17**, 107–112 (2004).
14. Pritchard, L. E., Tumbull, A. V. & White, A. Pro-opiomelanocortin processing in the hypothalamus: impact on melanocortin signaling and obesity. *J. Endocrinol.* **172**, 411–421 (2002).
15. Cone, R. D. Anatomy and regulation of the central melanocortin system. *Nature Neurosci.* **8**, 571–578 (2005).
16. Phillips, M. S. *et al.* Leptin receptor missense mutation in the fatty Zucker rat. *Nature Genet.* **13**, 18–19 (1996).

17. Fan, W. *et al.* Role of melanocortinergic neurons in feeding and the agouti obesity syndrome. *Nature* **385**, 165–168 (1997).
18. Mountjoy, K. G. *et al.* Localization of the melanocortin-4 receptor (MC4-R) neuroendocrine and autonomic control circuits in the brain. *Mol. Endocrinol.* **8**, 1298–1308 (1994).
19. Liu, H. *et al.* Transgenic mice expressing green fluorescent protein under the control of the melanocortin-4 receptor promoter. *J. Neurosci.* **23**, 7143–7154 (2003).
20. Butler, A. A. *et al.* Melanocortin-4 receptor is required for acute homeostatic response to increased dietary fat. *Nature Neurosci.* **4**, 605–611 (2005).
21. Taniguchi, N. *et al.* The postmitotic growth suppressor necdin interacts with a calcium-binding protein (NEFA) in neuronal cytoplasm. *J. Biol. Chem.* **275**, 31674–31681 (2000).
22. Satoh, T. *et al.* Activation of peroxisome proliferator-activated receptor- γ stimulates the growth arrest and DNA-damage inducible 153 gene in non-small cell lung carcinoma cells. *Oncogene* **21**, 2171–2180 (2002).
23. Tsuchiya, T., Shimizu, H., Horie, T. & Mori, M. Expression of leptin receptor in lung: leptin as a growth factor. *Eur. J. Pharmacol.* **365**, 273–279 (1999).
24. Oh-I, S. *et al.* Molecular mechanisms associated with leptin resistance: *n*-3 polyunsaturated fatty acids induce alterations in the tight junction of the brain. *Cell Metab.* **1**, 331–341 (2005).

Supplementary Information is linked to the online version of the paper at www.nature.com/nature.

Acknowledgements We thank M. Taguchi, M. Yoshida and E. Kada for technical assistance, and K. Yoshikawa and M. Kojima for supplying mouse NUCB2 cDNA and developing ELISA, respectively. This work was supported in part by grants-in-aid from the Ministry of Health, Labor and Welfare of Japan (to M. Mori).

Author Contributions S.O. and H.S. contributed equally to this work.

Author Information Reprints and permissions information is available at www.nature.com/reprints. The authors declare no competing financial interests. Correspondence and requests for materials should be addressed to M.M. (mmori@med.gunma-u.ac.jp).

Figure 1 | Expression of NUCB2 and nesfatin-1 in the rat hypothalamus. a–d, Immunohistochemical analysis. **a**, arcuate nucleus (Arc); **b**, PVN; **c**, supraoptic nucleus (SON); **d**, lateral hypothalamic area (LHA). 3V, third ventricle; f, (fornix); opt, (optic nerve). **e**, *In situ* hybridization with NUCB2 antisense cRNA. Zi, zona incerta. **f, g**, Food intake ($n=6-7$) after i.c.v. injection of NUCB2: **f**, dose–response; **g**, time course (open bars, 0 pmol NUCB2; filled bars, 4 pmol NUCB2). **h**, Double immunostaining with nesfatin Ab24 (4-Cl⁻naphthol in grey) and PC antibodies (Alexa594 in red) in the hypothalamus. **i, j**, Hypothalamic NUCB2 mRNA levels (**i**, $n=6-7$) and the PVN nesfatin-1 concentrations (**j**, $n=4$) in rats fed *ad libitum* (open bars) or starved for 24 h (filled bars). Data are means \pm s.e.m. Asterisk, $P<0.05$; two asterisks, $P<0.01$ compared with 0 pmol or *ad libitum* (Student's *t*-test).

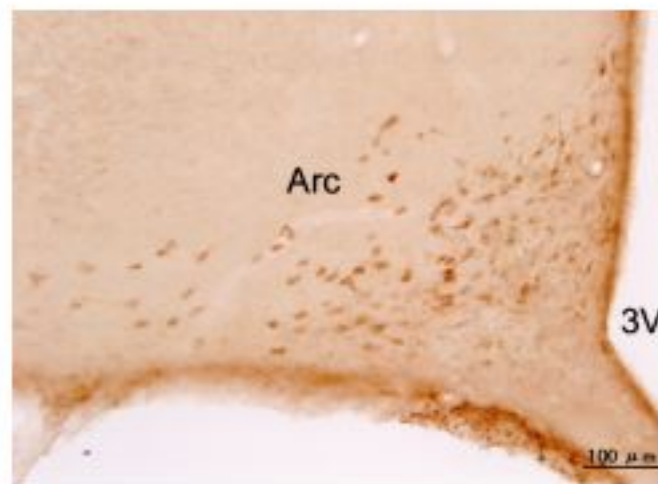
Figure 2 | Nesfatin-1-induced satiety in rats. a, b, Food intake ($n=5-8$) after i.c.v. injection of nesfatin-1; **a**, dose–response; **b**, time course (open bars, 0 pmol nesfatin-1; filled bars, 5 pmol nesfatin-1). **c, d**, Food intake ($n=5-10$) after i.c.v. injection of each fragment (25 pmol) derived from NUCB2: **c**, 0–1 h; **d**, 1–3 h. **e**, Food intake ($n=5-7$) after i.c.v. injection of 8 μ g IgG (open bars, control rabbit IgG; red bars, nesfatin Ab24 IgG; black bars, nesfatin Ab301 IgG). **f–h**, Food intake ($n=5-6$) after i.c.v. injection of each intermediate (5 pmol) with wild-type Lys 83-Arg 84 (WT) or mutant Ala 83-Ala 84 (Mut). **f**, 0–1 h; **g**, 1–3 h; **h**, 3–6 h. Data are means \pm s.e.m. Asterisk, $P<0.05$; two asterisks, $P<0.01$ compared with 0 pmol, vehicle (V) or control IgG.

Figure 3 | Body weight changes after continuous i.c.v. injection of substances. a, b, Daily food intake (**a**) and body weight gain (**b**; increment from Day 0) in rats ($n=4-5$) after nesfatin-1 injection (5 pmol daily). Open squares, vehicle; filled squares, nesfatin-1. **c, d**, Daily food intake (**c**) and body weight gain (**d**, increment from Day 0) in rats ($n=4-5$) after injection with NUCB2 missense (open squares) or antisense (filled squares) morpholino oligonucleotide (MON; 40 μ g per day). Antisense (5'-ATGGTCCTCCACCTCATCTTCAGAG-3') and 5-missense (5'-ATCGTGCTCCACGTCATCTACACAG-3') MONs were purchased from Gene Tools. An Alzet osmotic mini-infusion pump was used for continuous injection. Data are means \pm s.e.m. Asterisk, $P<0.05$; two asterisks, $P<0.01$ compared with vehicle or missense MON.

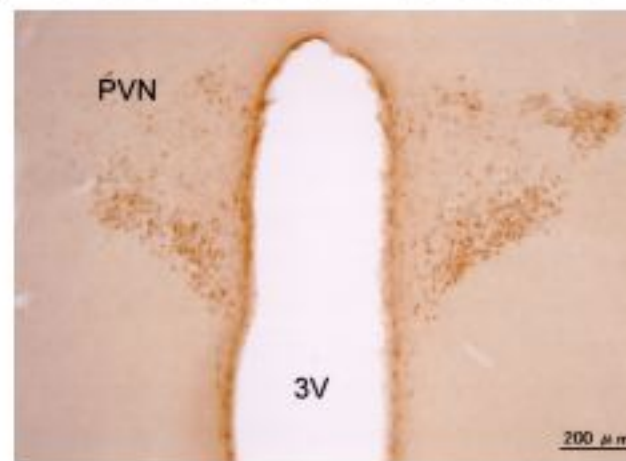
Figure 4 | Nesfatin-1-induced satiety associated with leptin or melanocortin signaling. **a, b**, Food intake in lean (**a**) and Zucker (**b**) rats ($n=5$) after i.c.v. injection of 5 pmol nesfatin-1 (open bars, vehicle; filled bars, nesfatin-1). **c**, Effects of nesfatin Ab24 on leptin-induced anorexia ($n=6$). Vehicle, 5 pmol nesfatin-1 or 5 pmol leptin was centrally administered 15 min after i.c.v. injection of Ab24 IgG (8 μ g) during the dark phase. **d, e**, Effects of SHU9119 on nesfatin-1-induced anorexia ($n=6$). Vehicle or 5 pmol nesfatin-1 was centrally administered 15 min after i.c.v. injection of 20 pmol SHU9119. Data are means \pm s.e.m. Asterisk, $P<0.05$; two asterisks, $P<0.01$ compared with vehicle.

Fig. 1

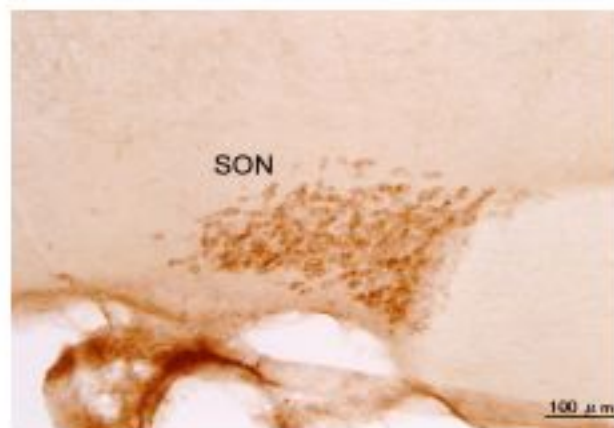
(a) Arcuate nucleus (Arc)



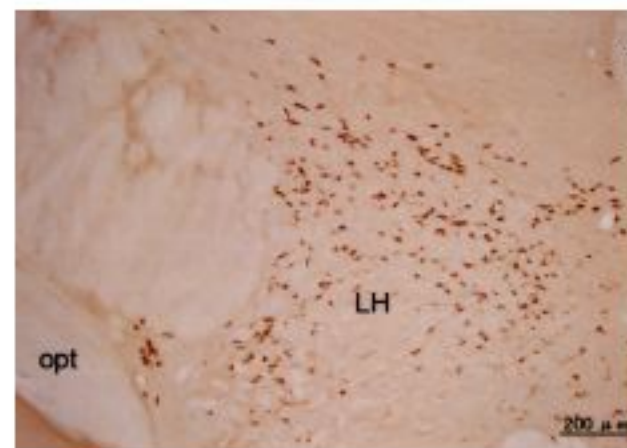
(b) Paraventricular nucleus (PVN)



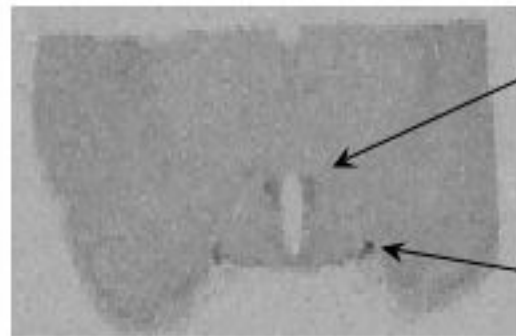
(c) Supraoptic nucleus (SON)



(d) Lateral hypothalamic area (LHA)

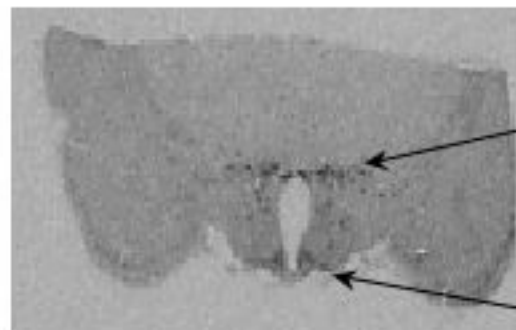


(e)



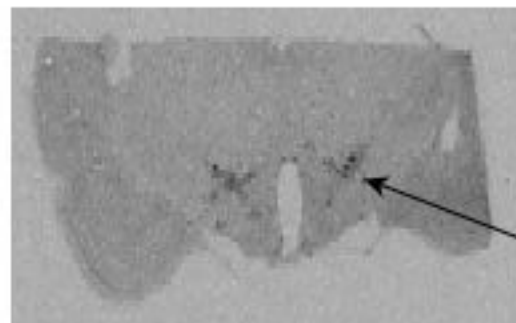
**Paraventricular
nucleus (PVN)**

**Supraoptic
nucleus (SON)**

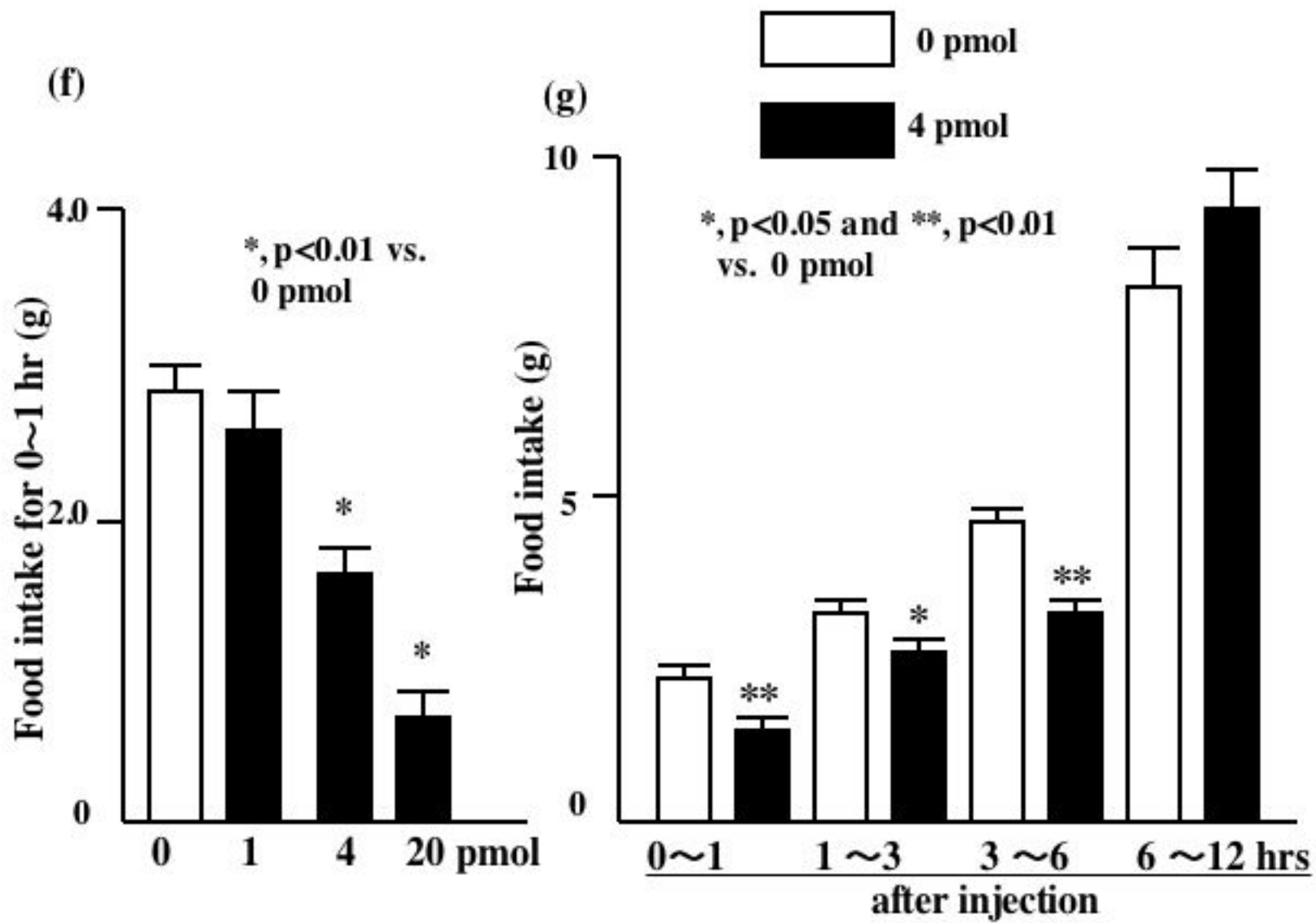


**Zona
incerta (Zi)**

**Arcuate
nucleus (Arc)**

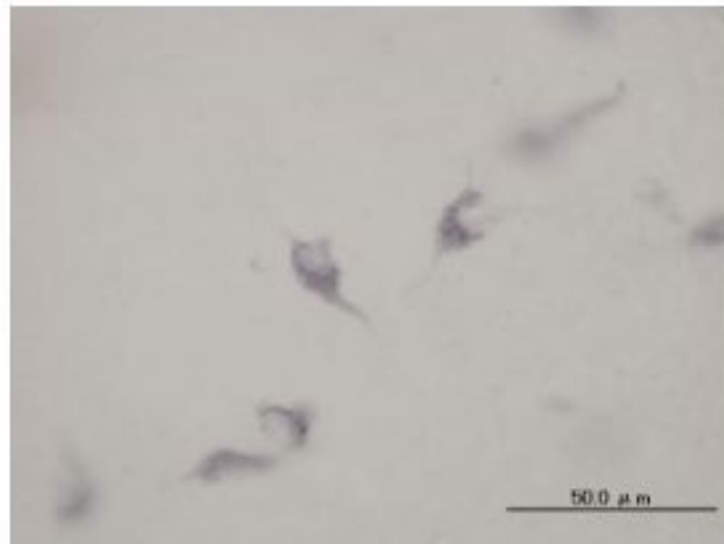


**Lateral hypothalamic
area (LHA)**

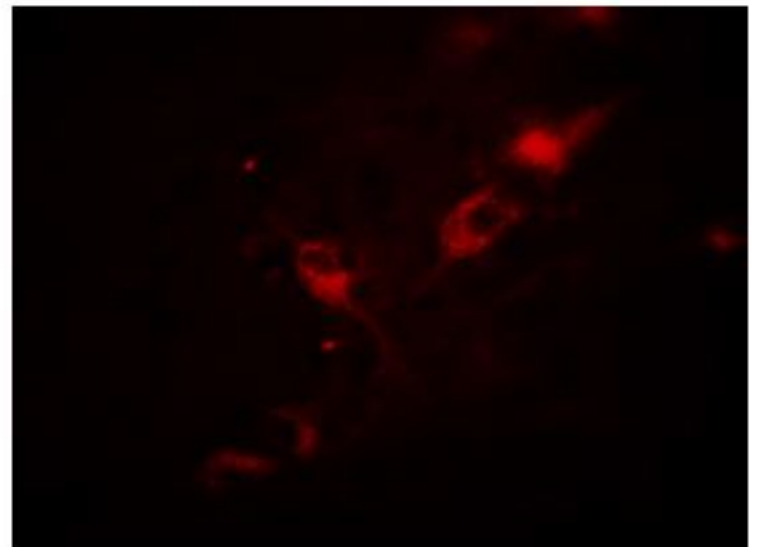


(h)

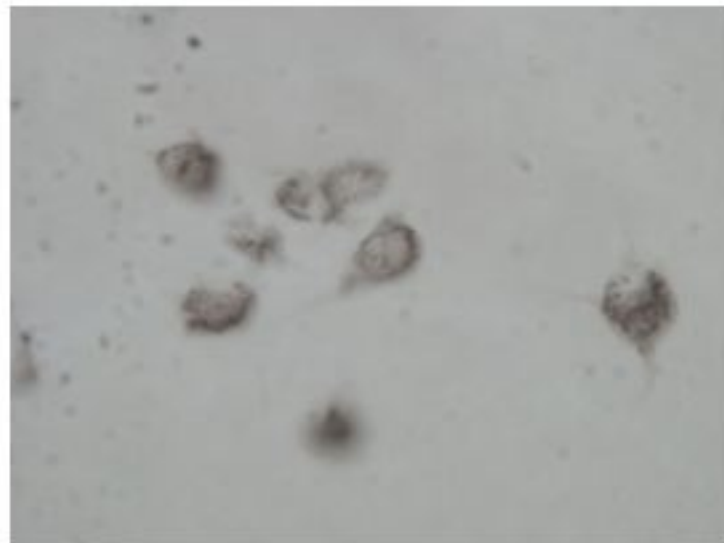
Nesfatin Ab 24



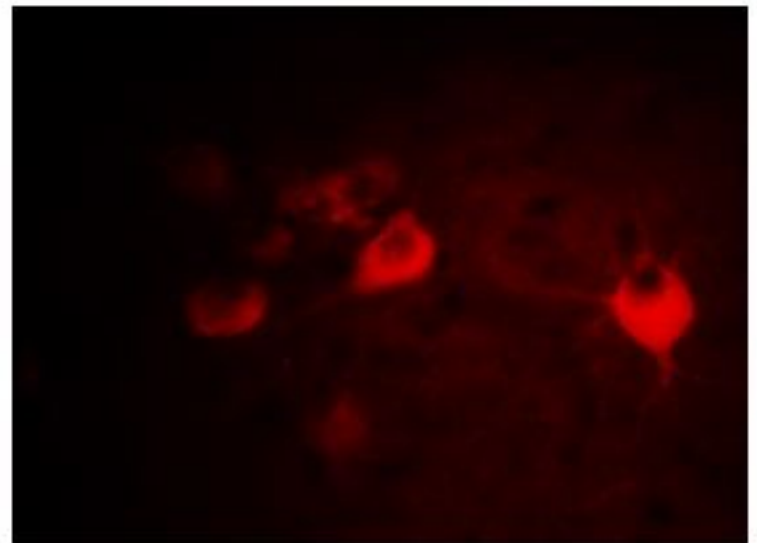
PC-3/1 antibody



Nesfatin Ab 24



PC-2 antibody



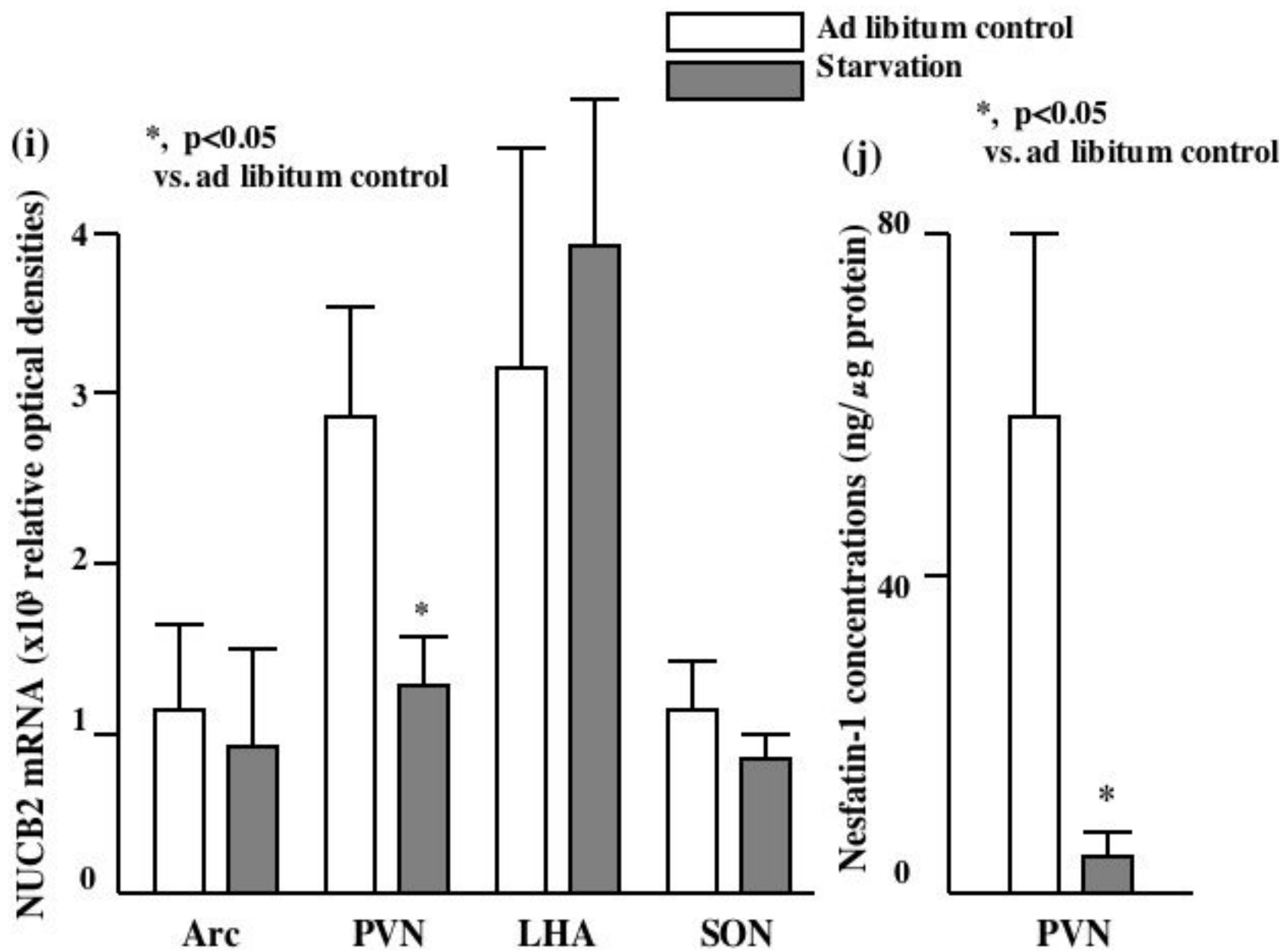
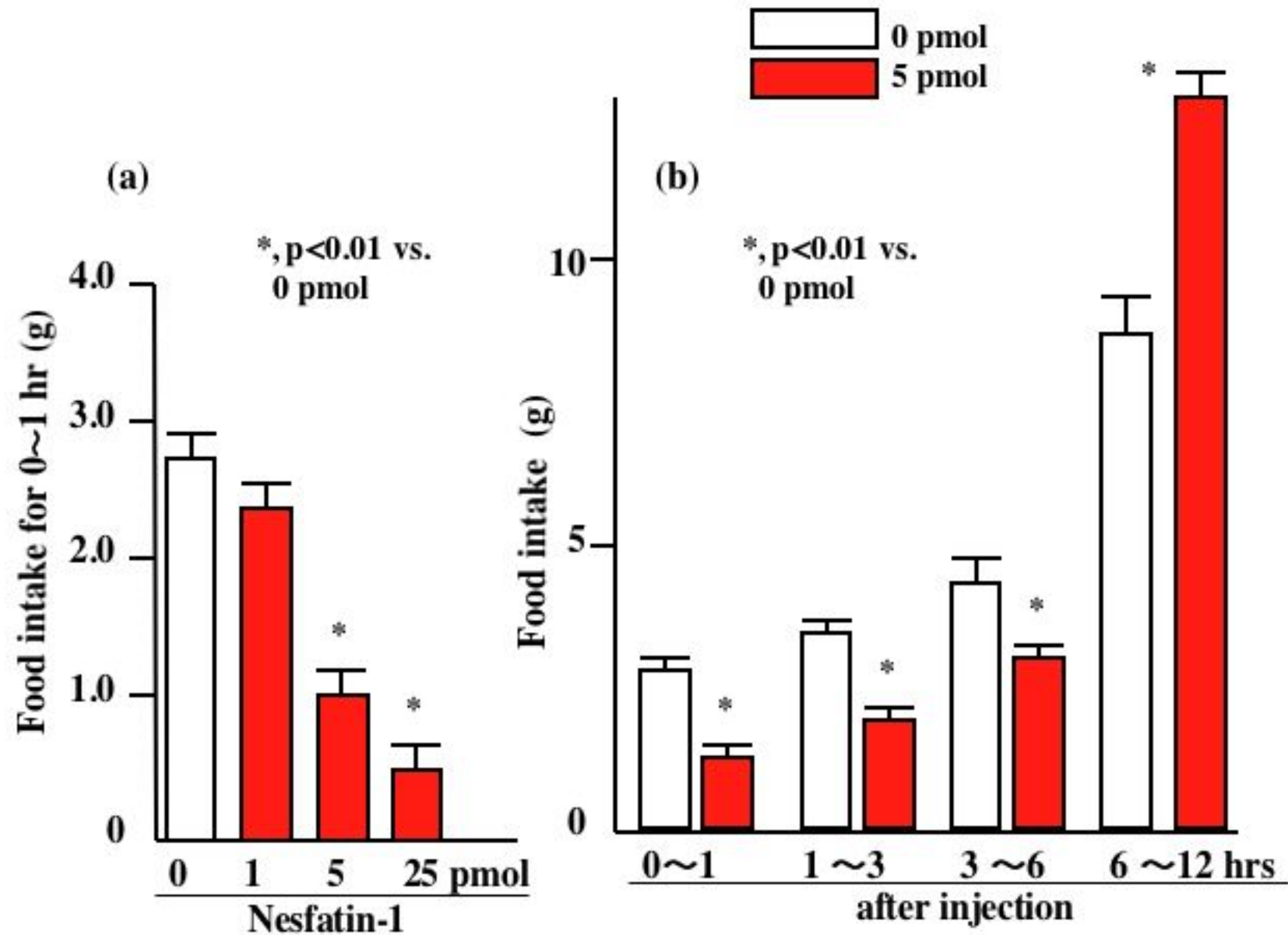
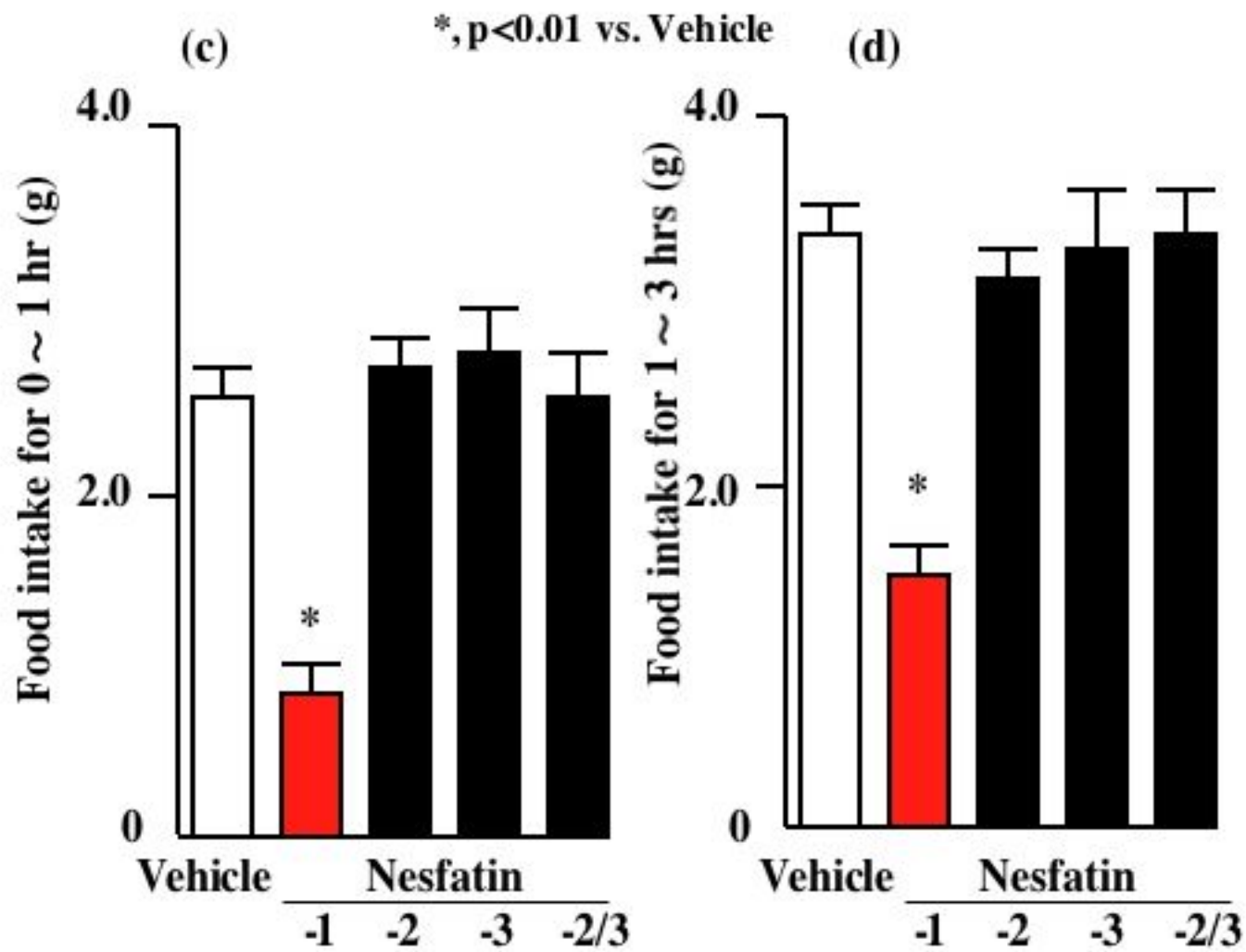
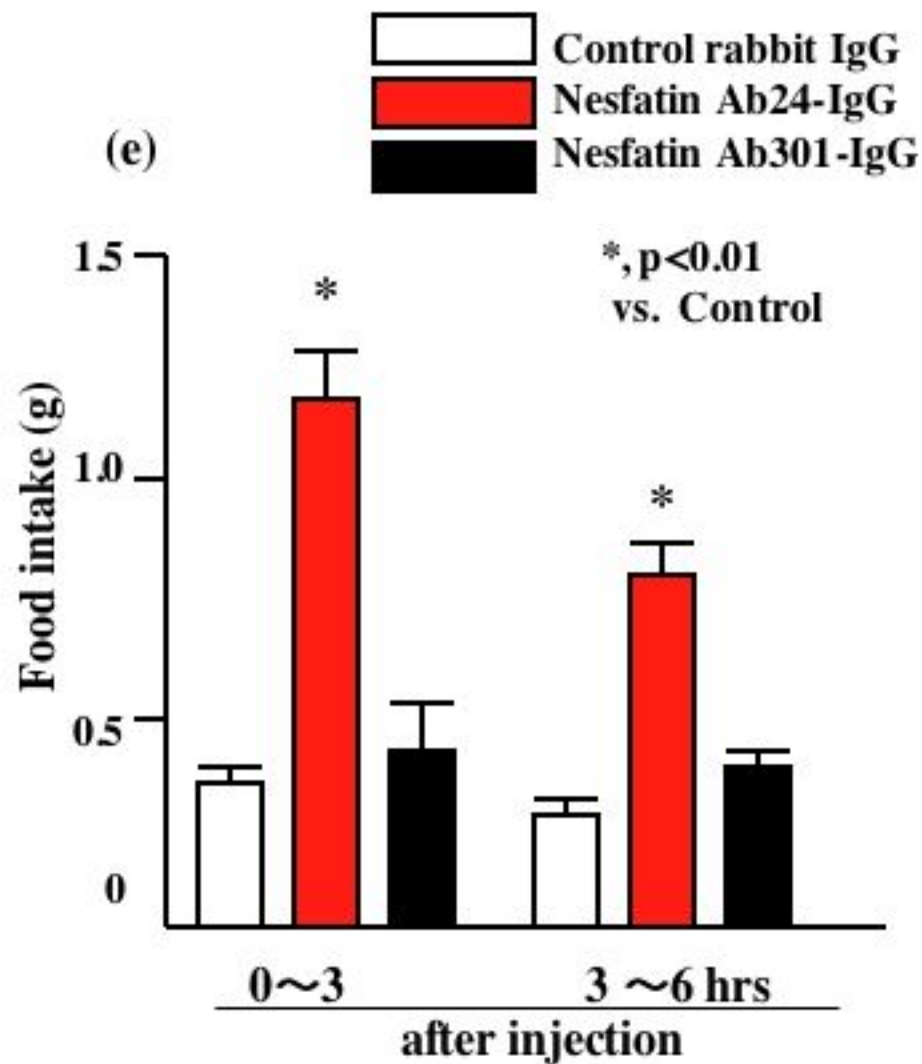


Fig. 2







***, p<0.01 vs. Vehicle**

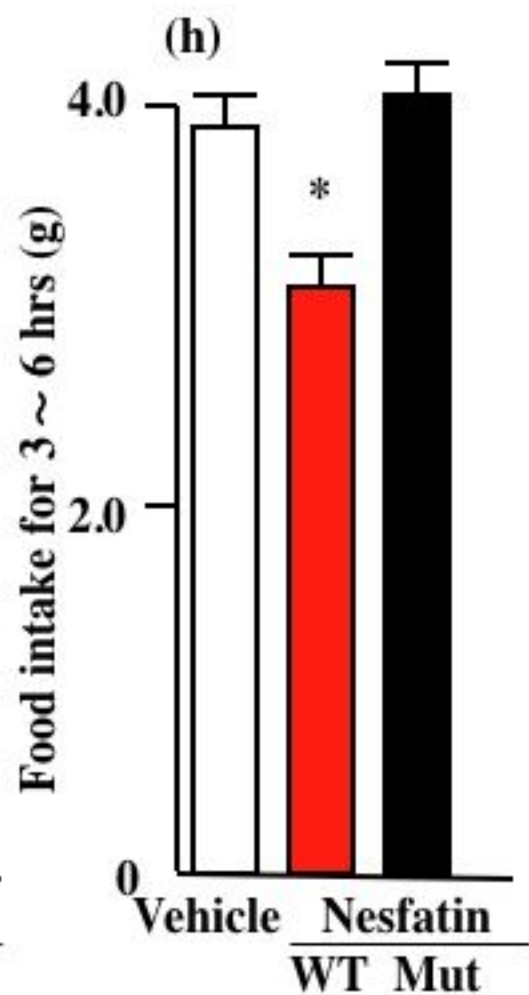
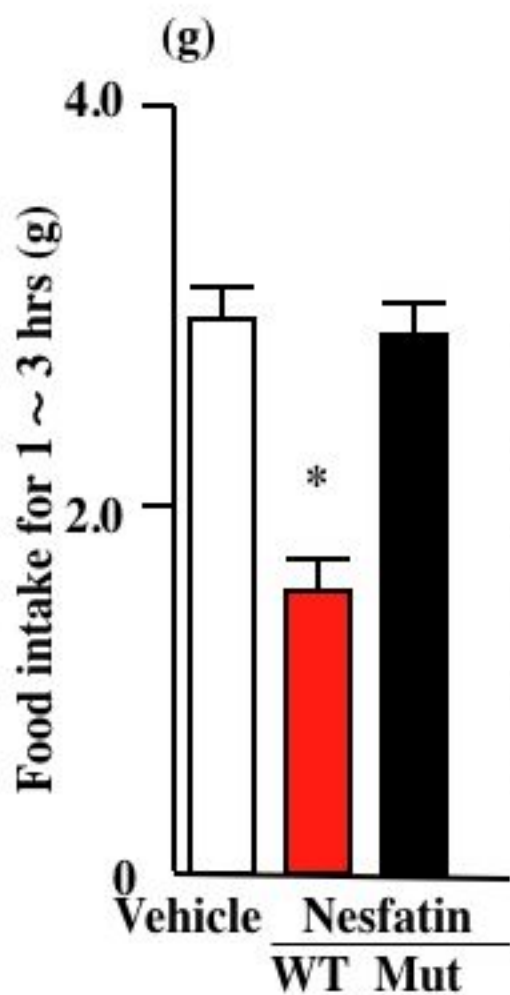
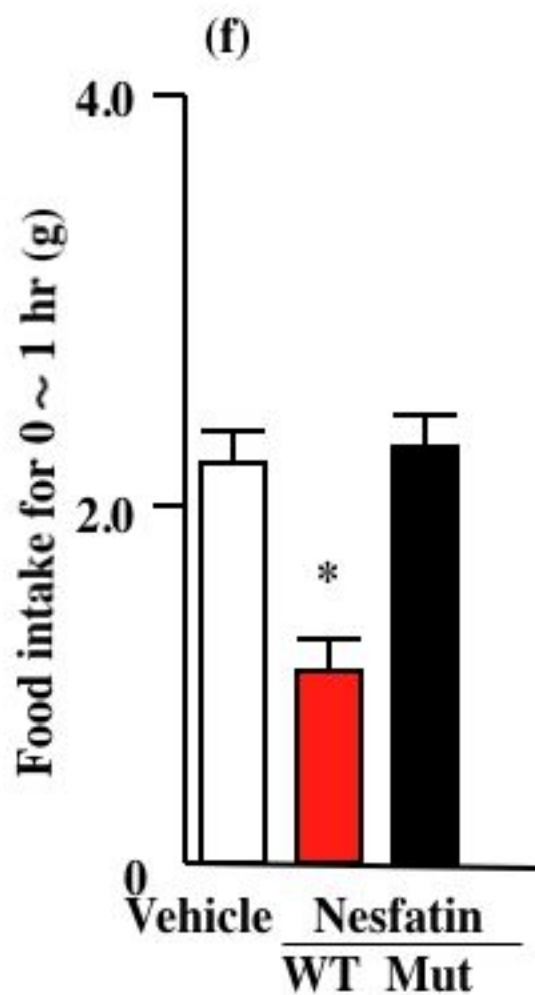
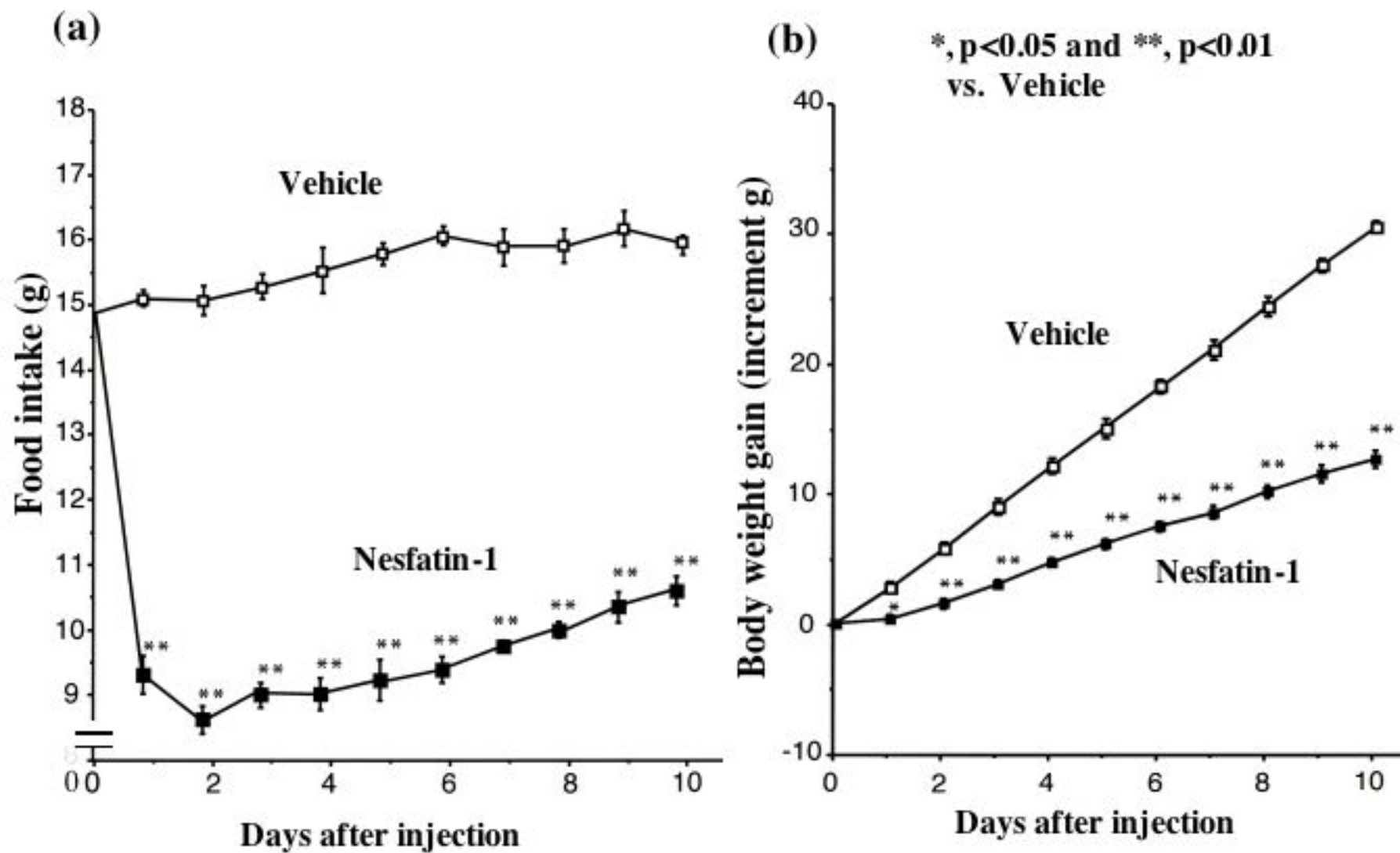


Fig. 3



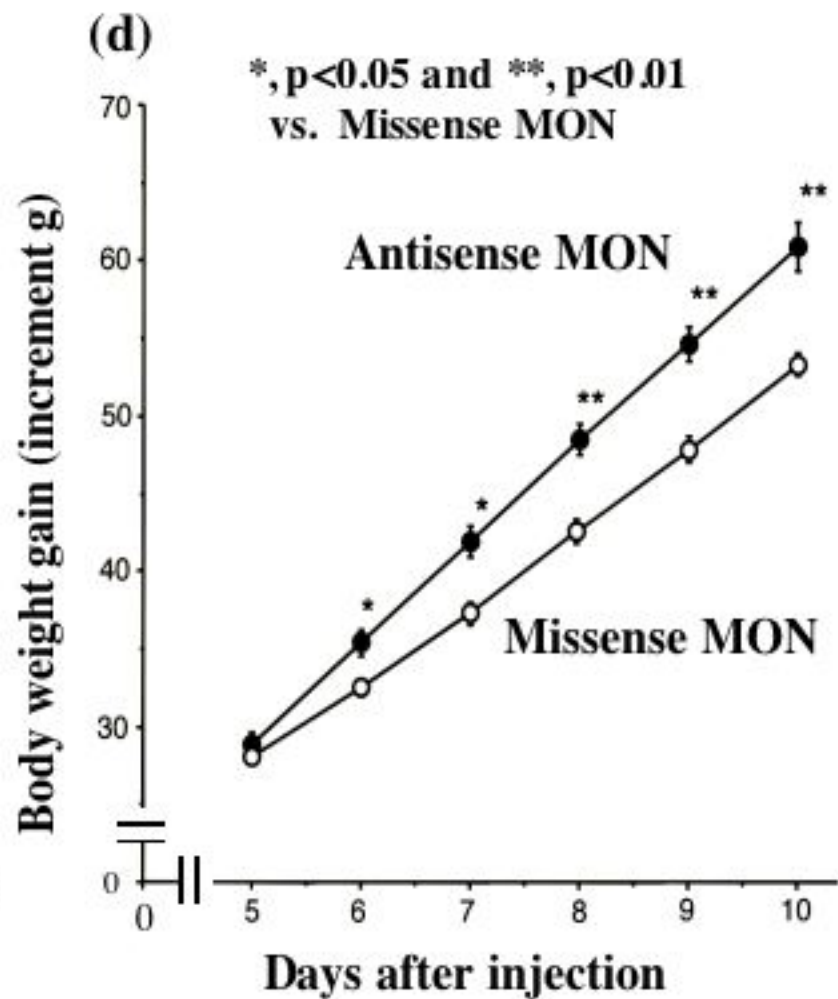
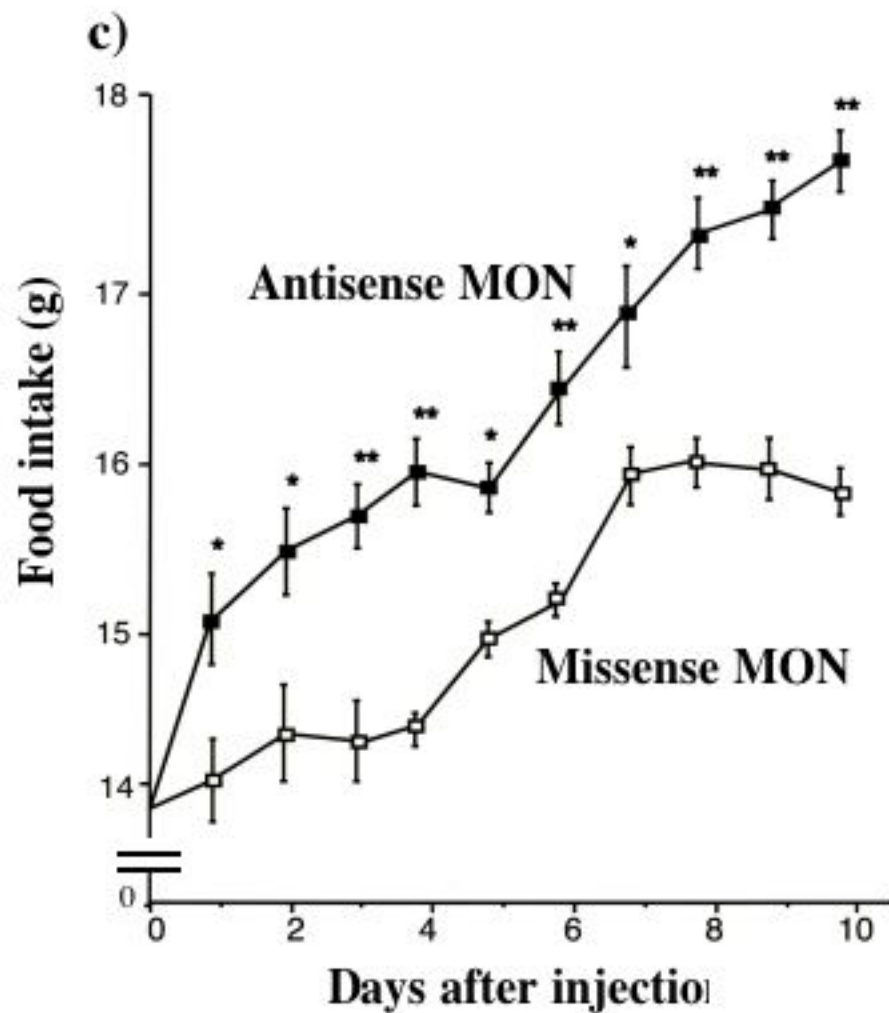
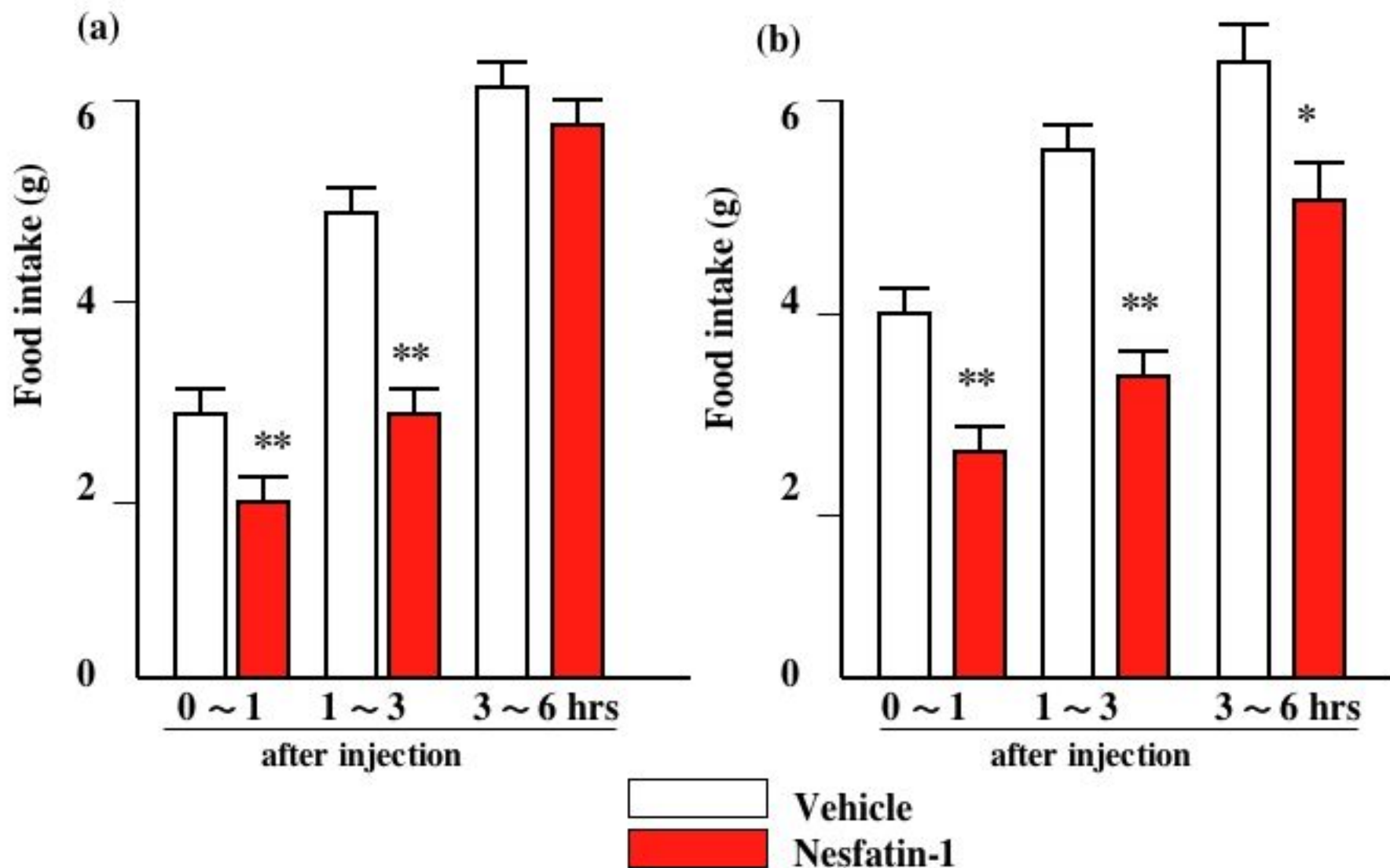
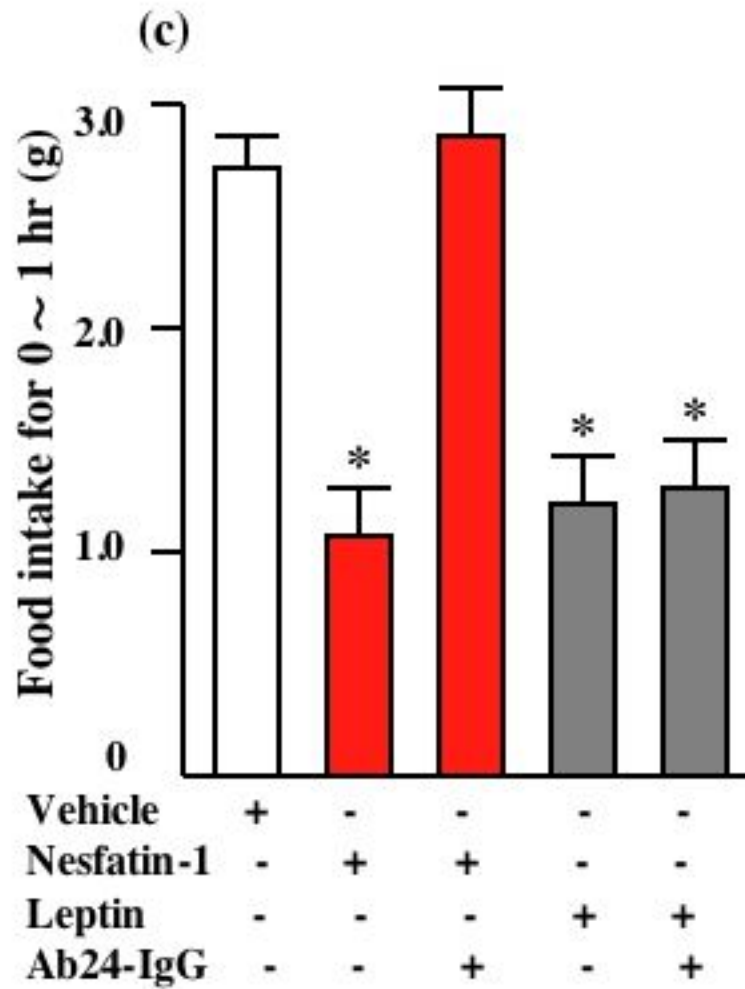


Fig. 4

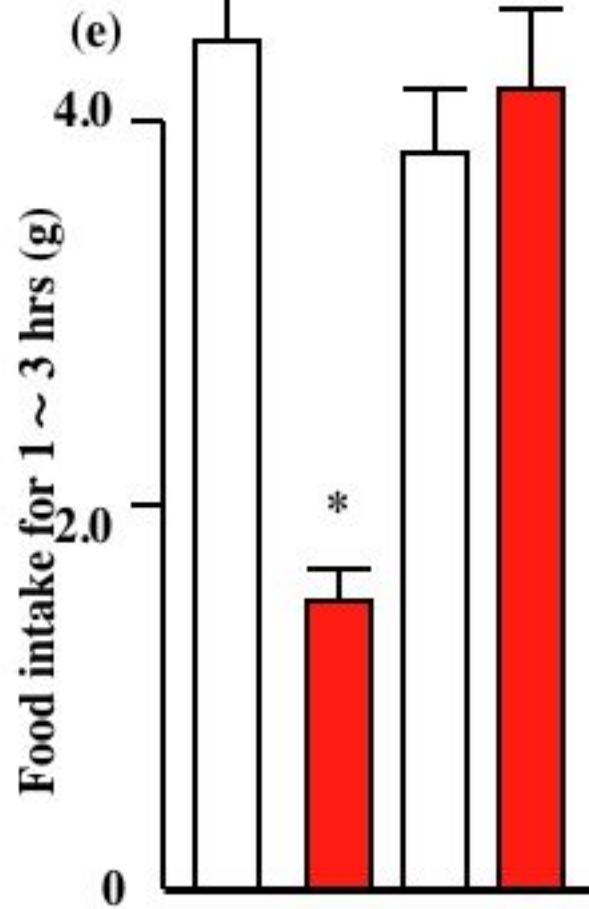
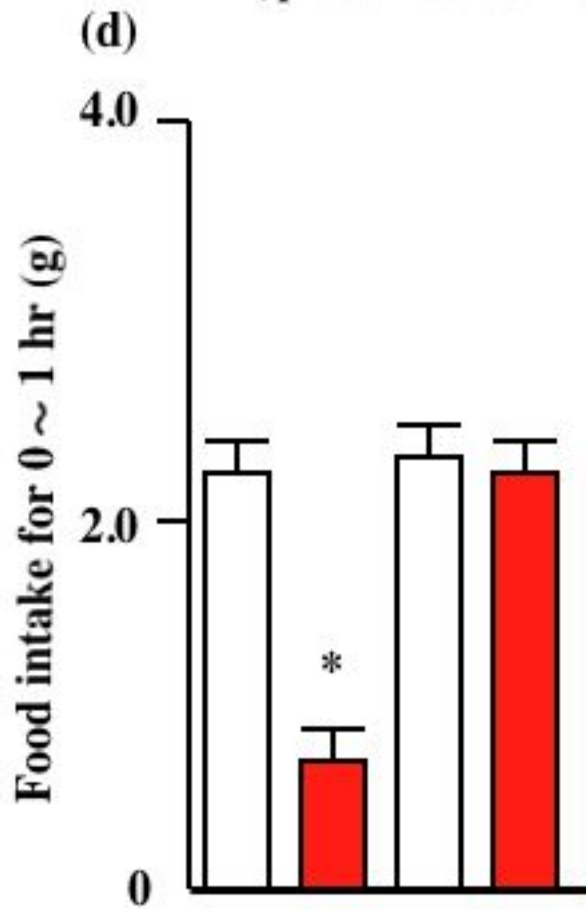
***, p<0.05 and **, p<0.01 vs. Vehicle**



***, p<0.01 vs. Vehicle**

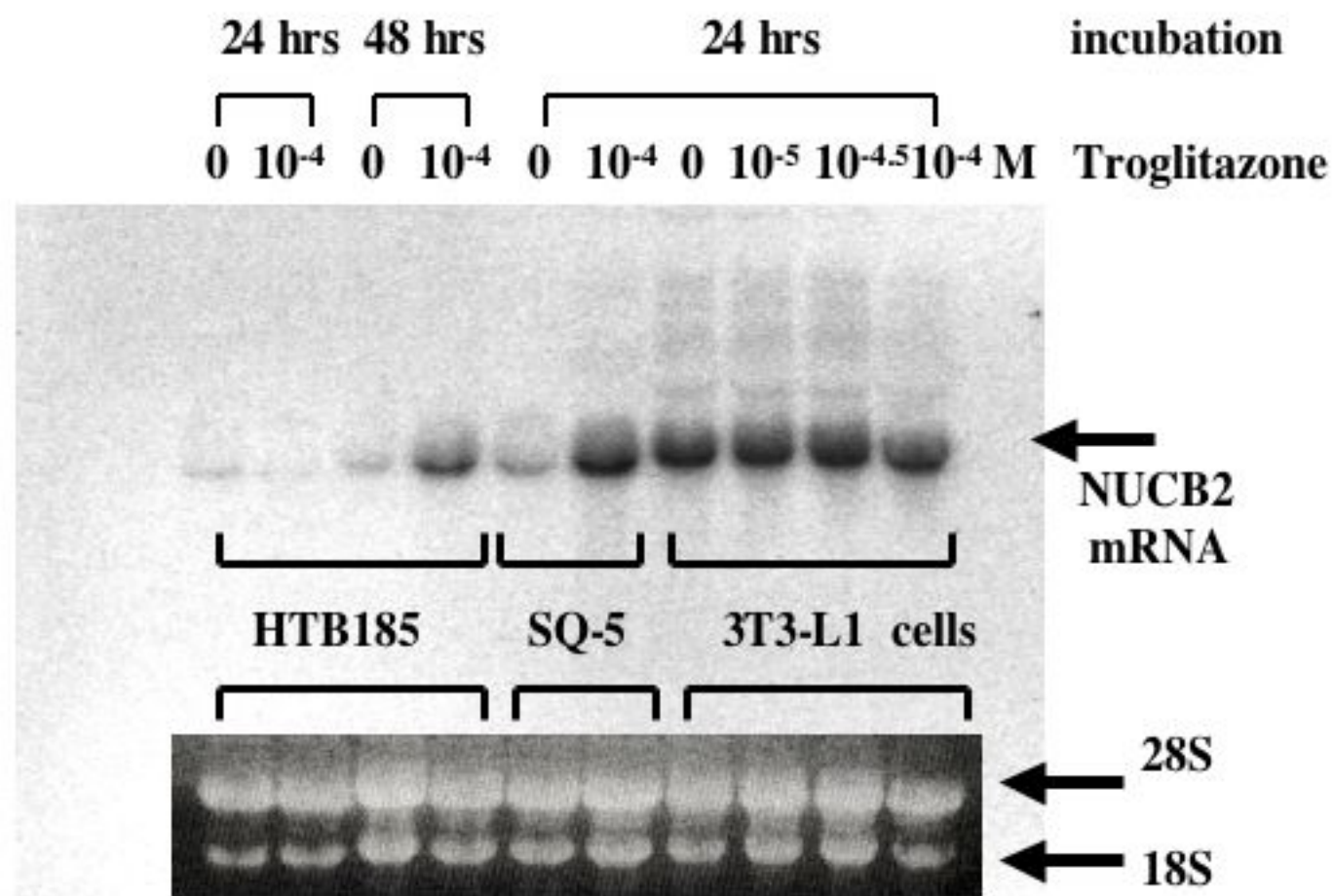


***, p<0.01 vs. Vehicle**

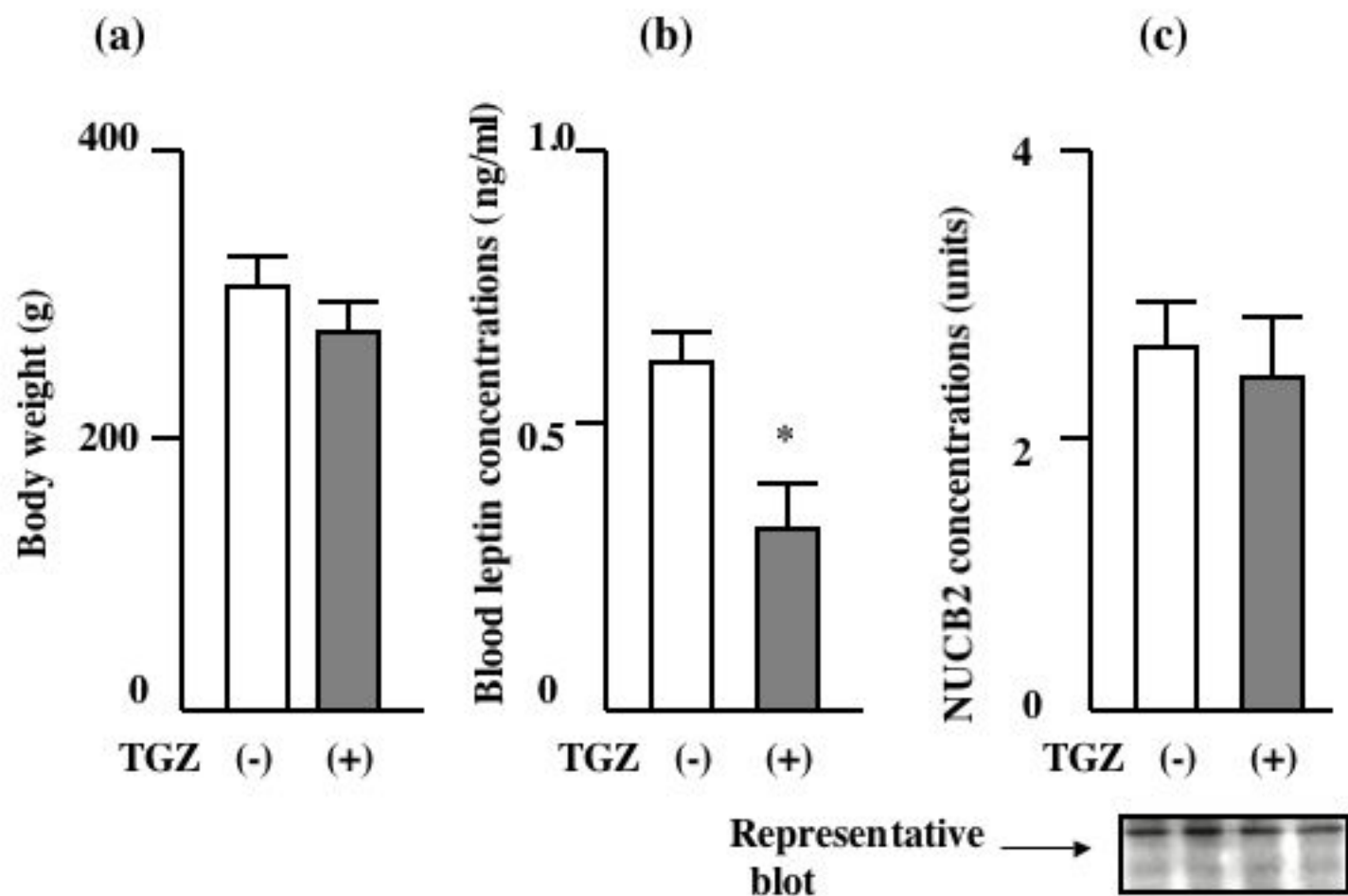


Vehicle	+	-	+	-
Nesfatin-1	-	+	-	+
SHU9119	-	-	+	+

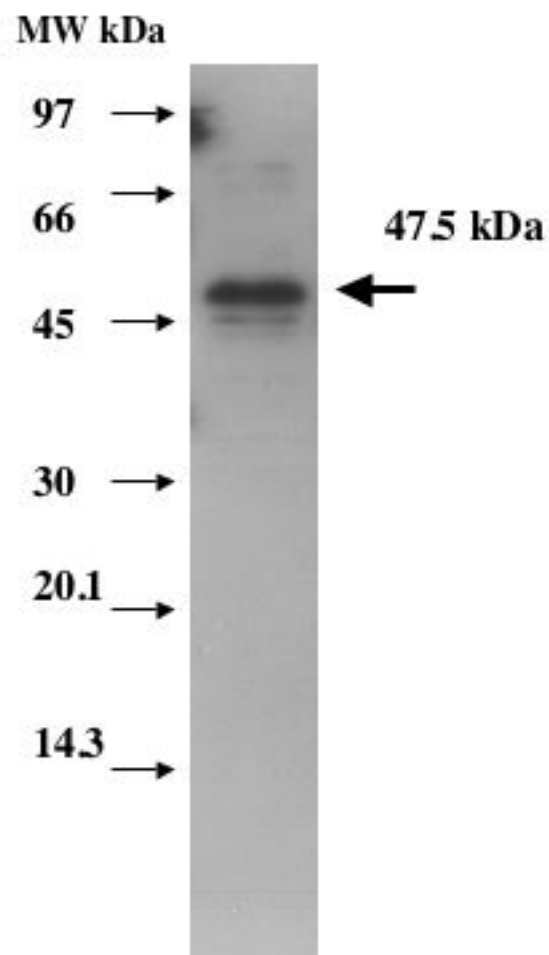
Supplementary Fig. 1



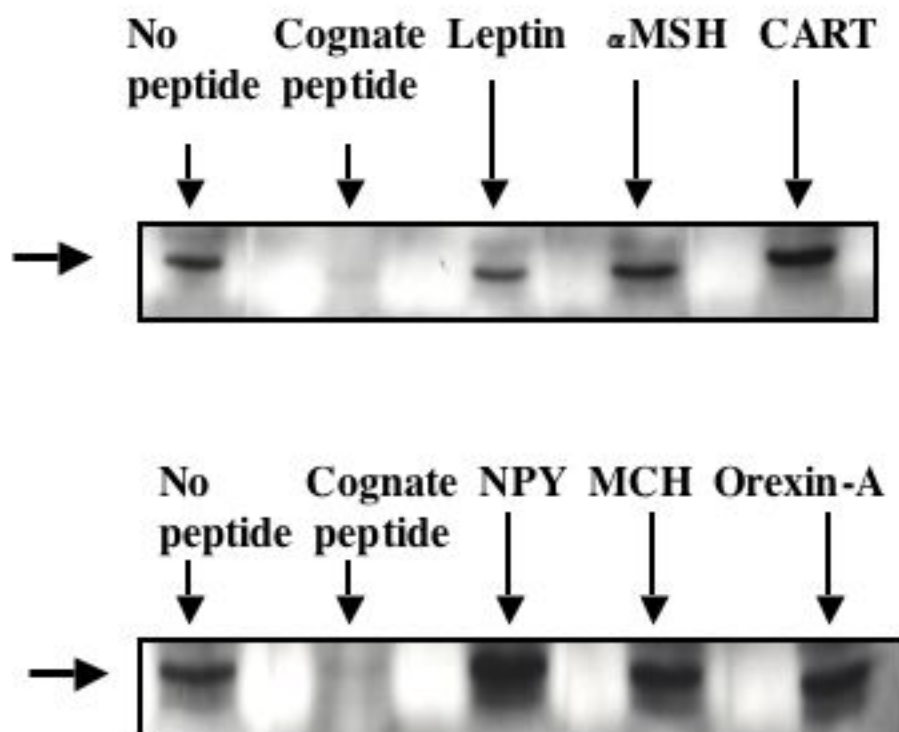
Supplementary Fig. 2



Supplementary Fig. 3

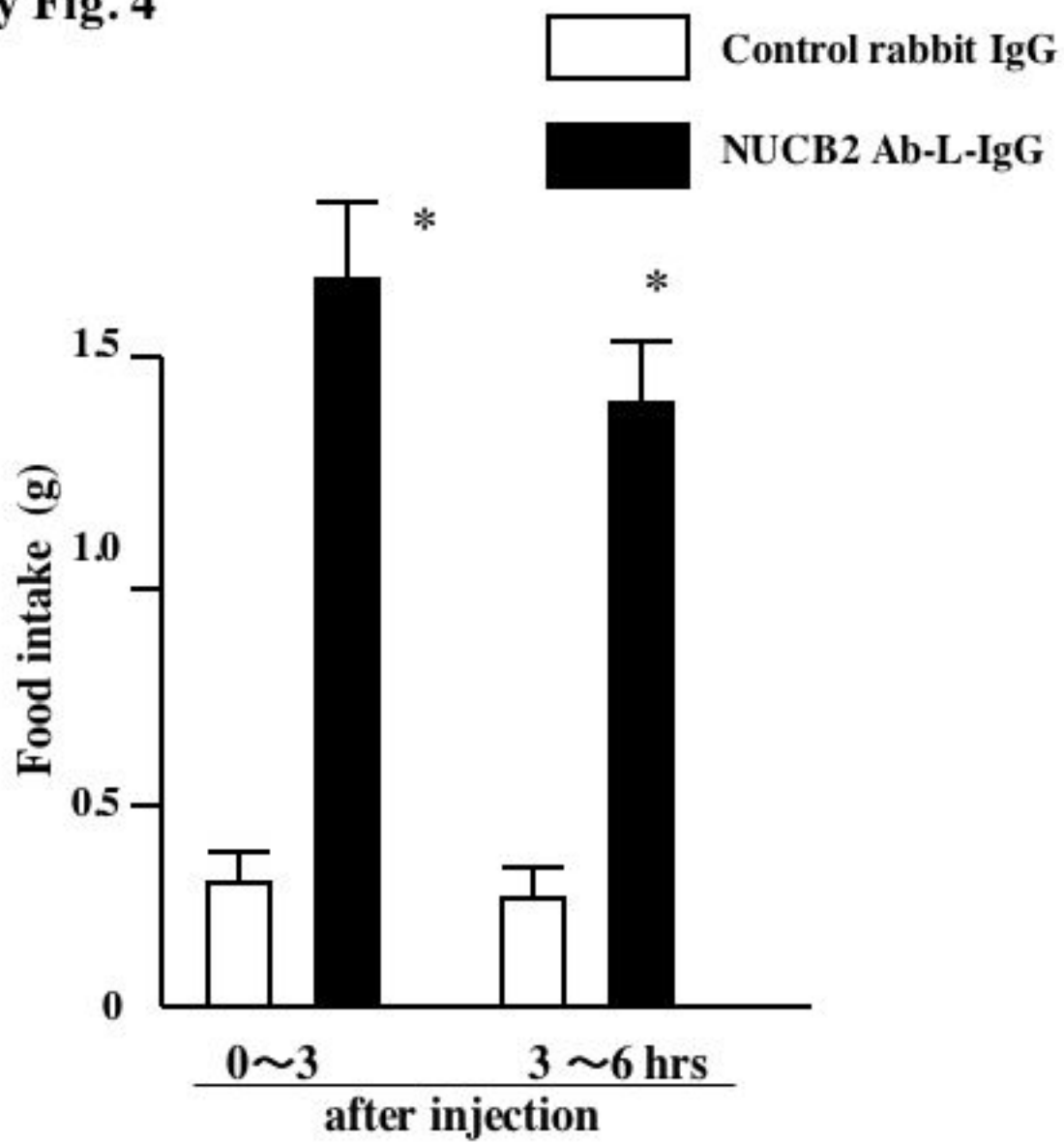


12% polyacrylamide gel



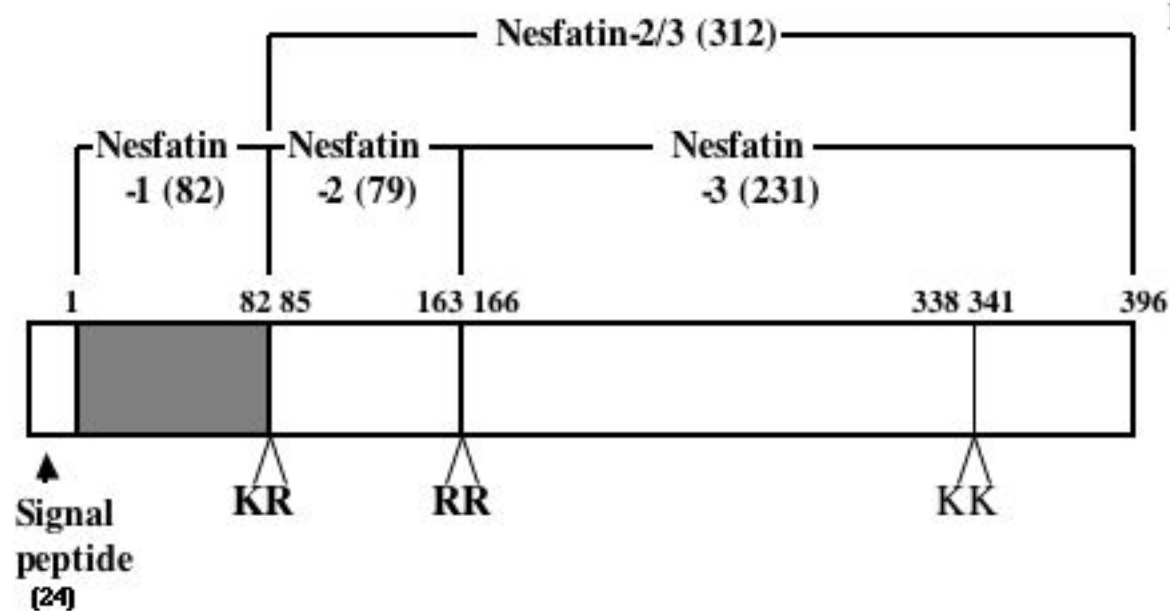
12% polyacrylamide gel

Supplementary Fig. 4



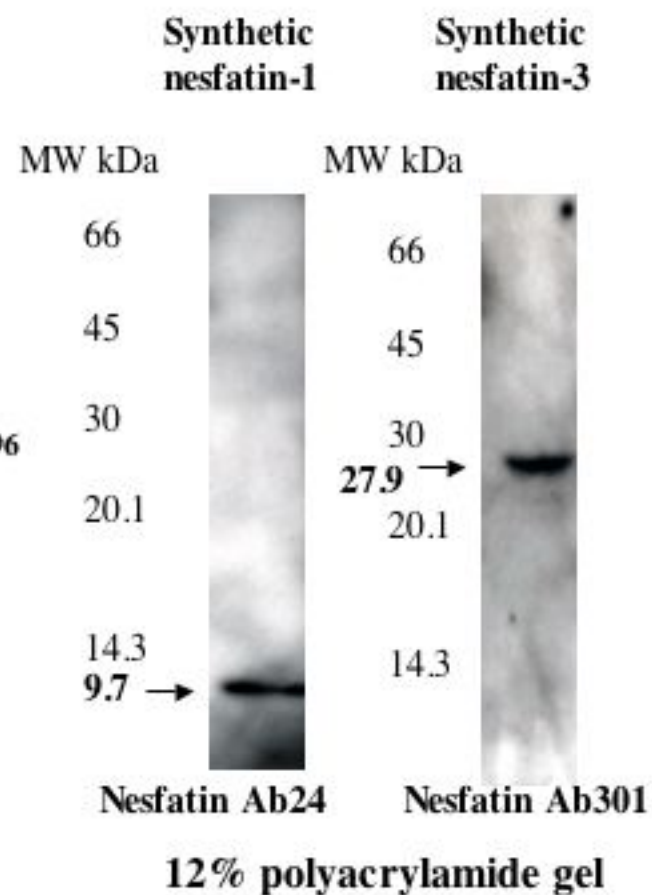
Supplementary Fig. 5

Putative processing sites



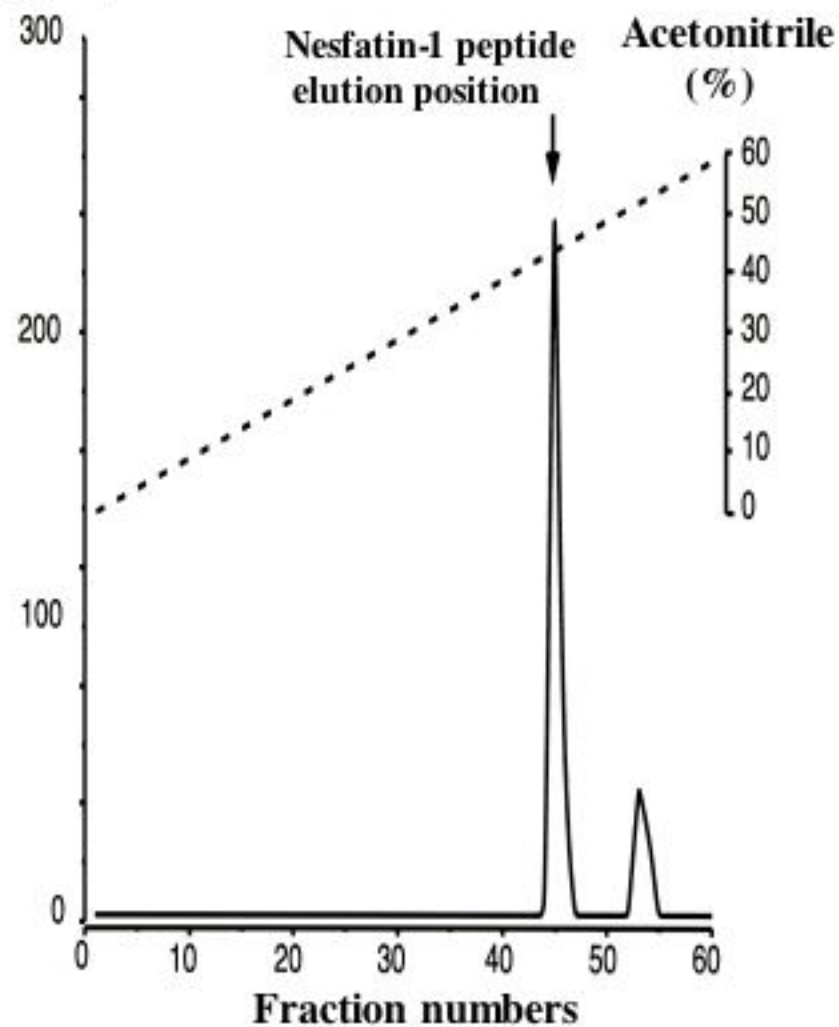
(), numbers of amino acids

Western blot

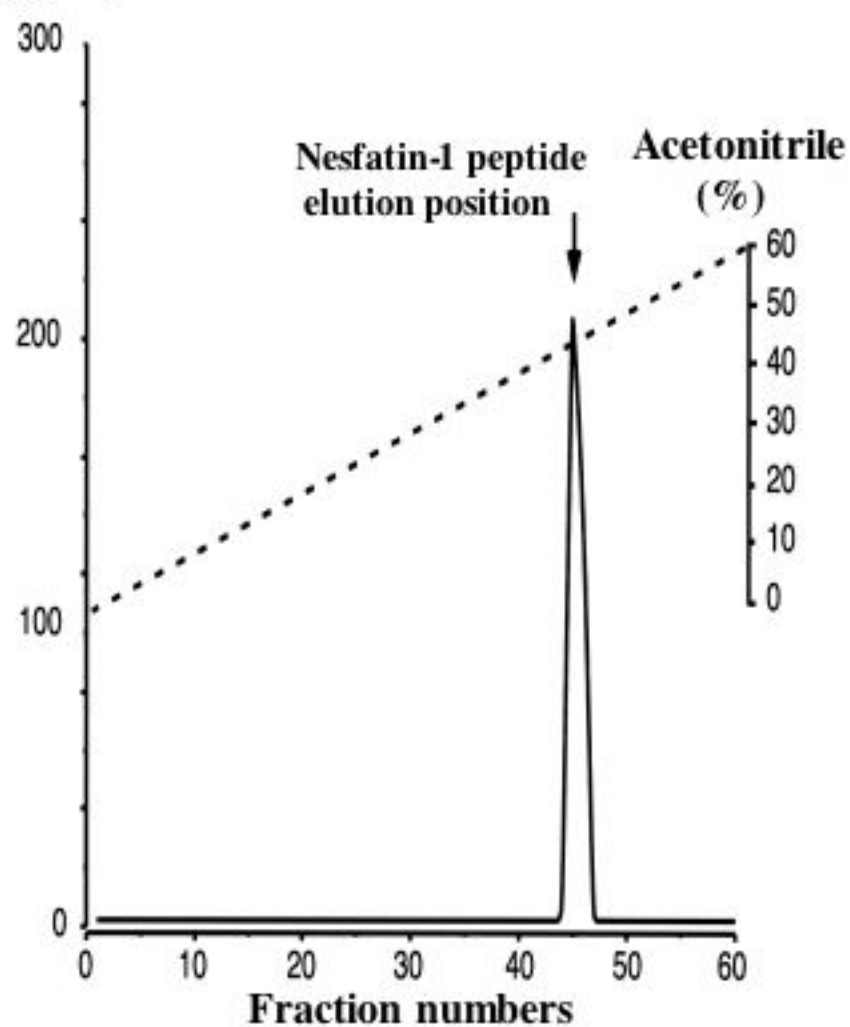


Supplementary Fig. 6

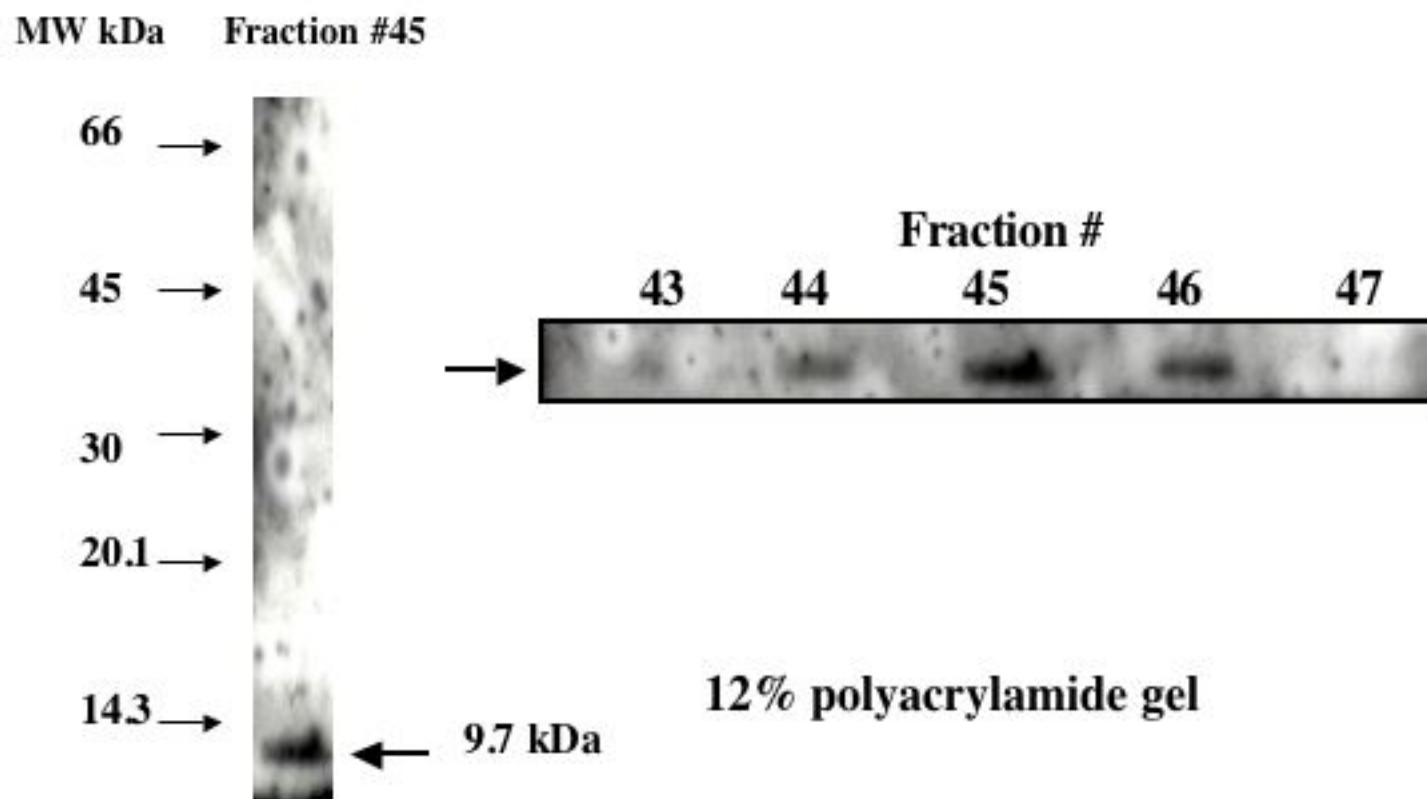
Nesfatin-1 (a)
(ng/ml)



Nesfatin-1 (b)
(ng/ml)



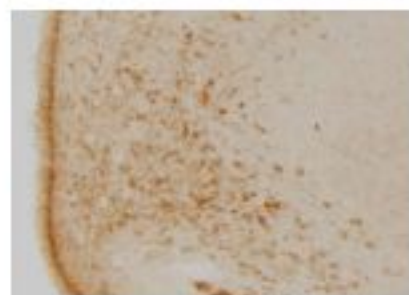
Supplementary Fig. 7



Supplementary Fig. 8

Arcuate nucleus

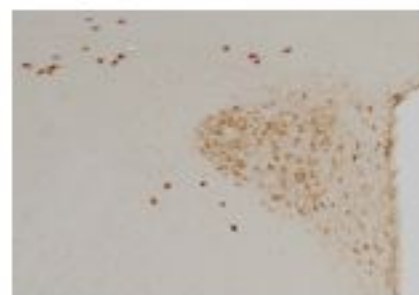
Paraventricular nucleus



Nesfatin Ab24



Nesfatin Ab24 + nesfatin-1



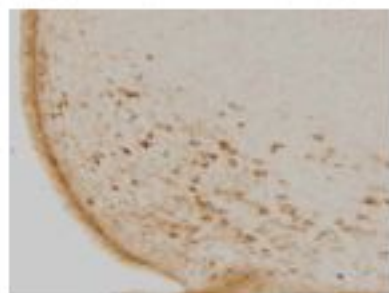
Nesfatin Ab24



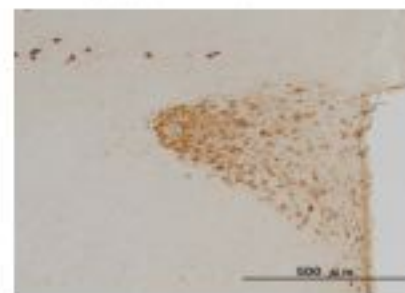
Nesfatin Ab24 + nesfatin-1



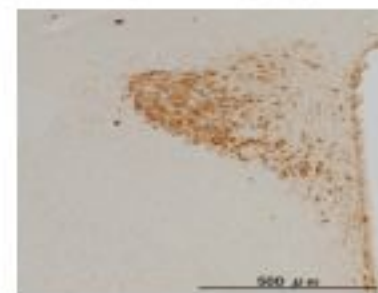
Nesfatin Ab24 + Leptin



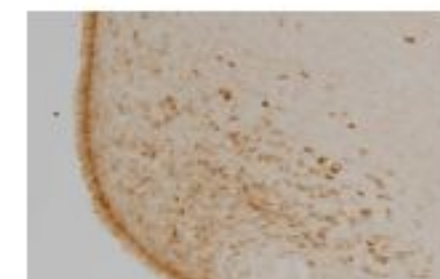
Nesfatin Ab24 + alpha-MSH



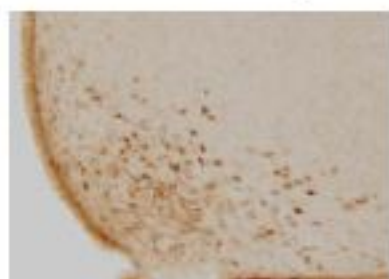
Nesfatin Ab24 + Leptin



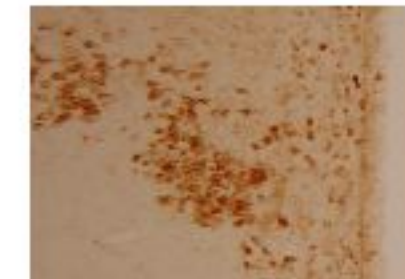
Nesfatin Ab24 + alpha-MSH



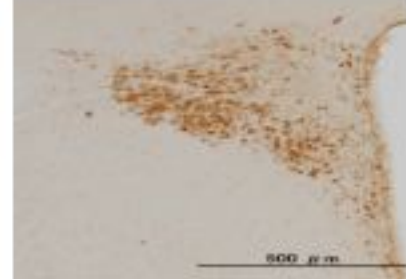
Nesfatin Ab24 + CART



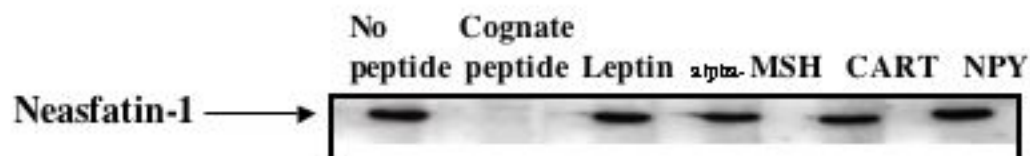
Nesfatin Ab24 + NPY



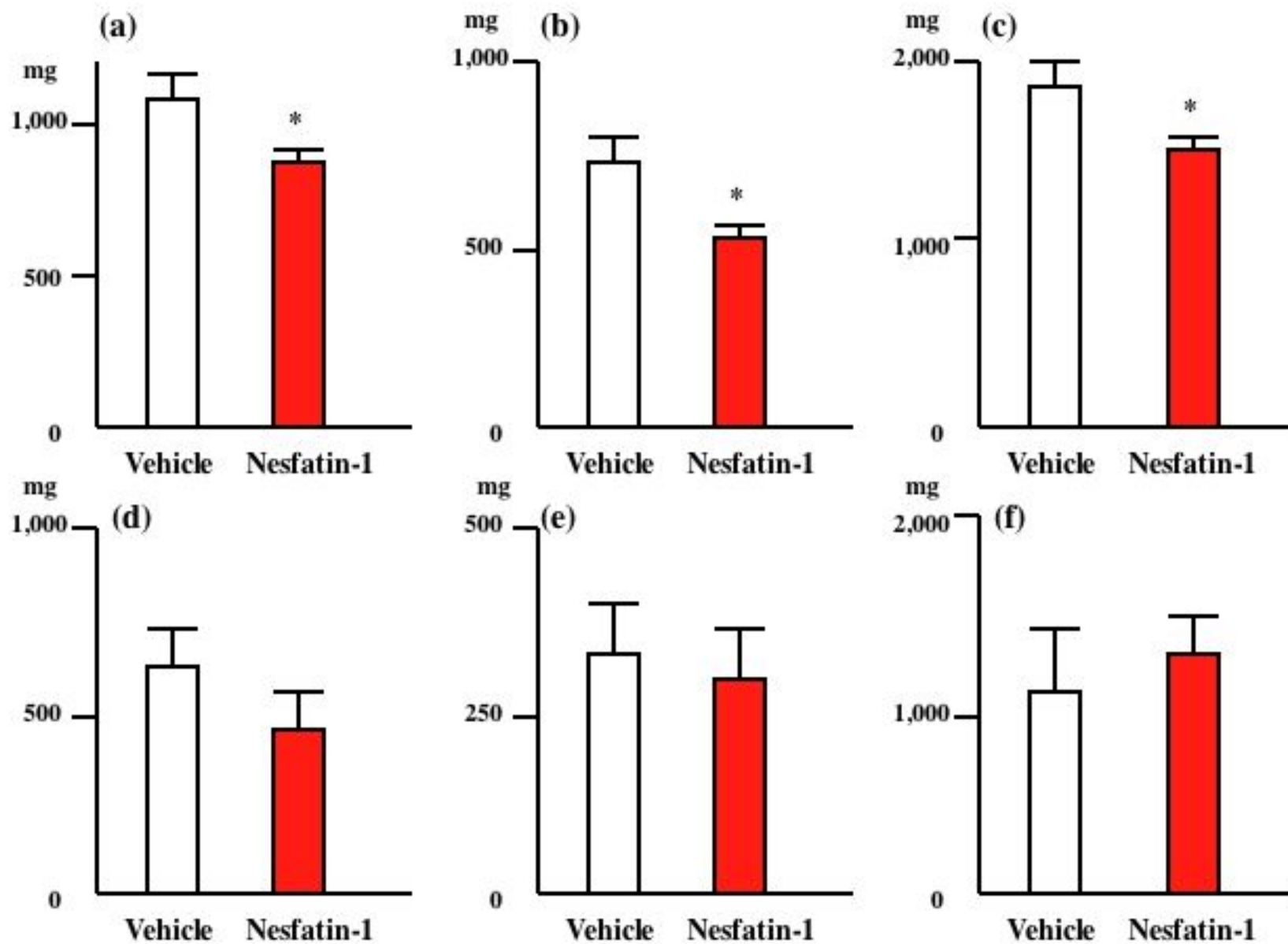
Nesfatin Ab24 + CART



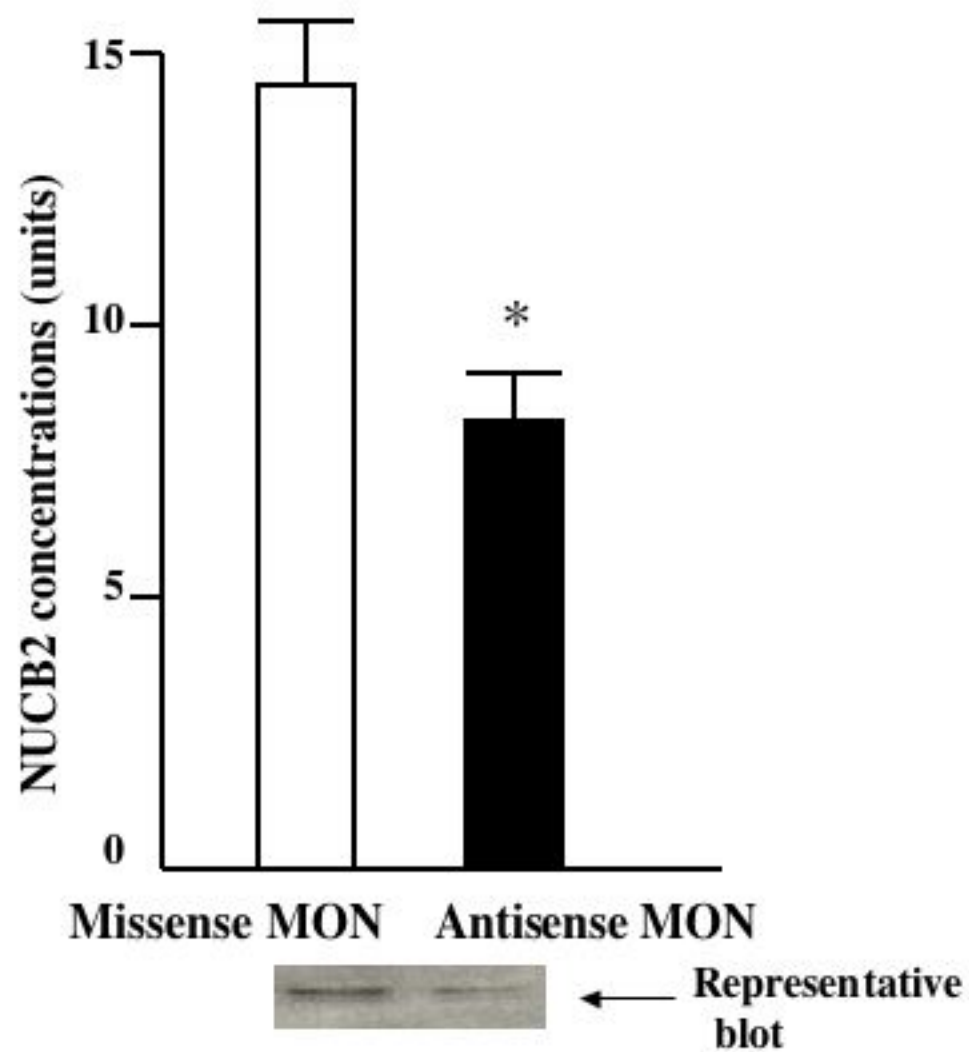
Nesfatin Ab24 + NPY



Supplementary Fig. 9

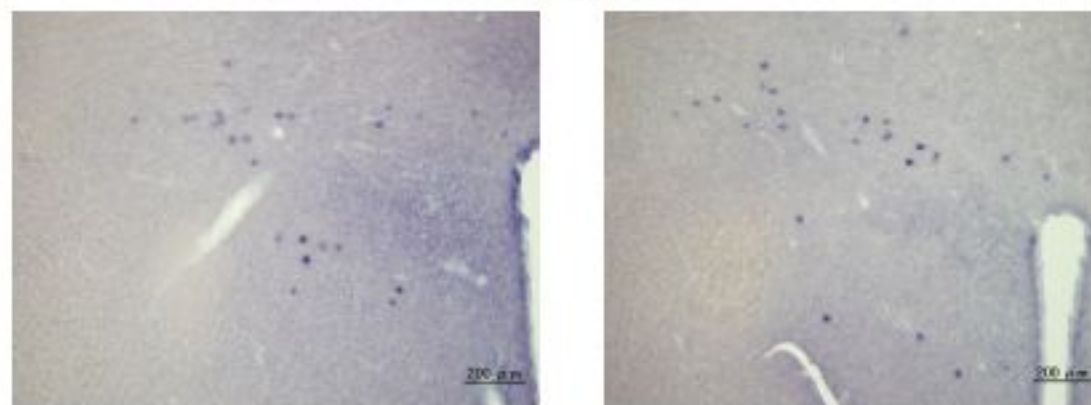


Supplementary Fig. 10



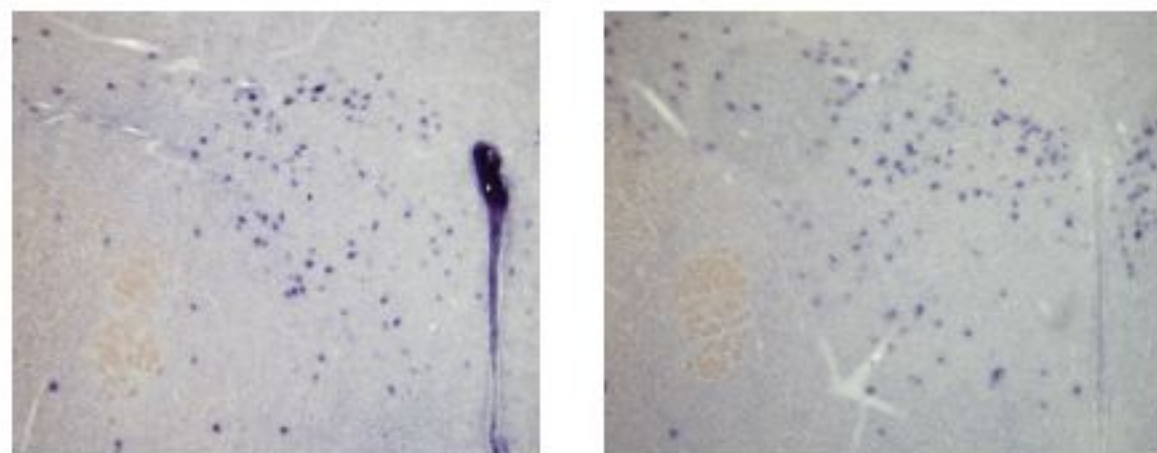
Supplementary Fig. 11

(a) NUCB2 (antisense)



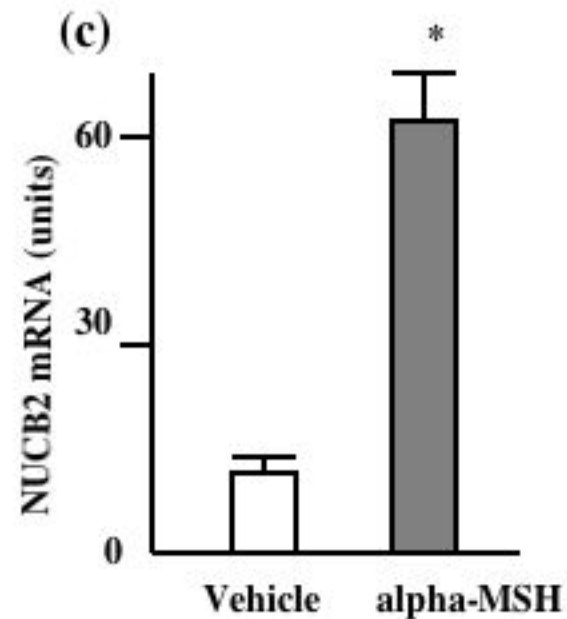
Vehicle injection

(b) NUCB2 (antisense)



alpha-MSH injection

(c)



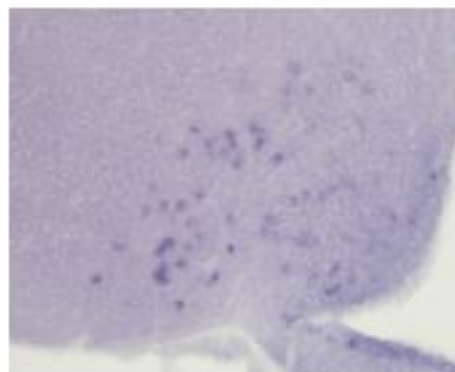
NUCB2 (sense)



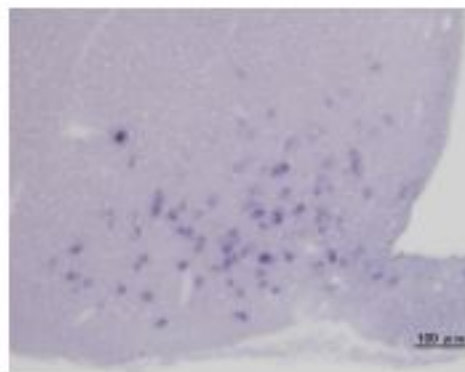
Supplementary Fig. 12



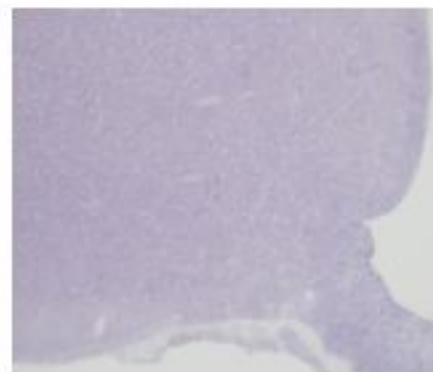
(a) POMC (antisense)
Vehicle injection



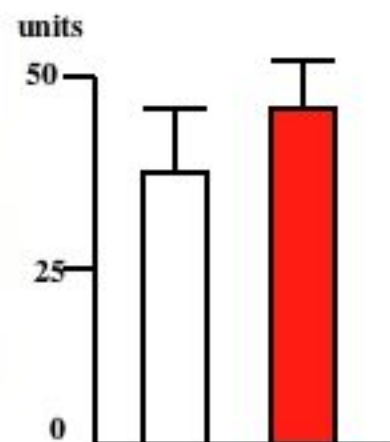
(b) POMC (antisense)
Nesfatin-1 injection



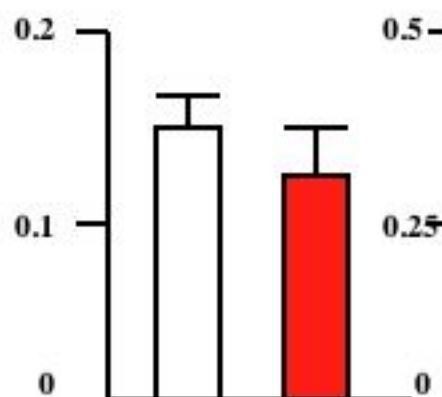
(c) POMC (sense)



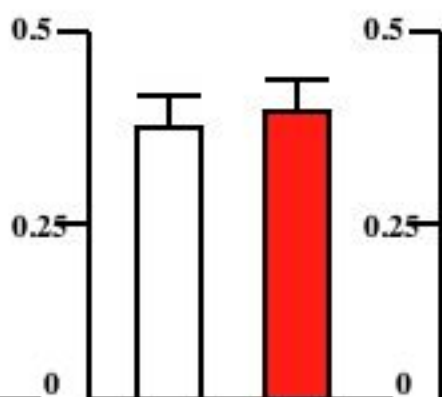
(d) POMC in Arc



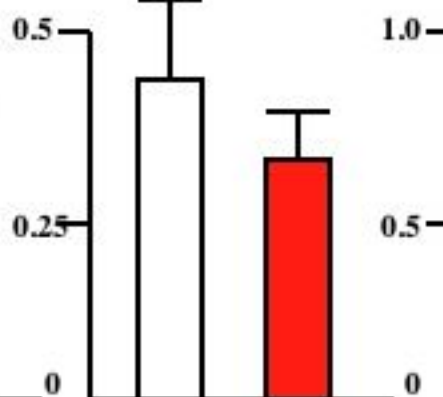
(e) POMC in PVN



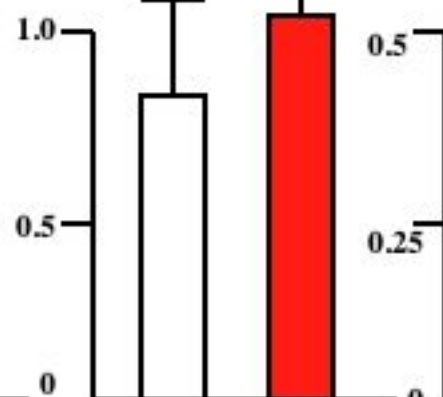
(f) AgRP in Arc



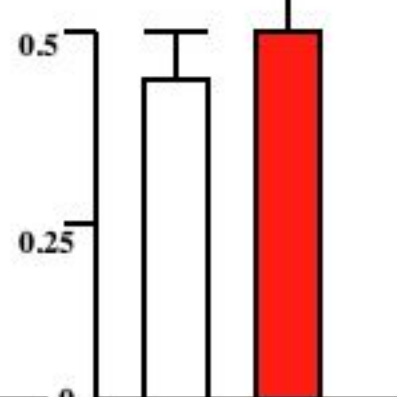
(g) AgRP in PVN



(h) NPY in Arc



(i) CRH in PVN



Supplementary Fig. 13

(S-14-1)
cAMP formation
(10³ pmol/well)

